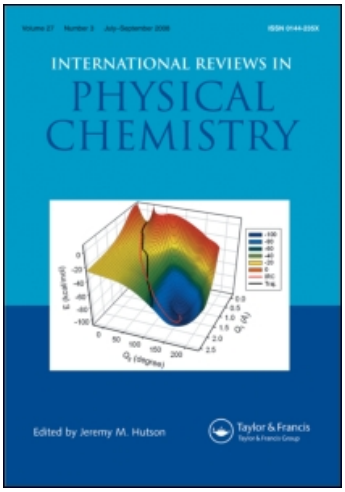

International Reviews in Physical Chemistry
Publication details, including instructions for authors and subscription information:
http://www.informaworld.com/smpp/title~content=t713724383

Experimental measurements of state resolved, rotationally inelastic energy transfer

Aram Schiffman[a]; David W. Chandler[a]
[a] Sandia National Laboratories, Livermore, CA, USA

To cite this Article Schiffman, Aram and Chandler, David W.(1995) 'Experimental measurements of state resolved, rotationally inelastic energy transfer', International Reviews in Physical Chemistry, 14: 2, 371 — 420
To link to this Article: DOI: 10.1080/01442359509353315
URL: http://dx.doi.org/10.1080/01442359509353315

INTERNATIONAL REVIEWS IN PHYSICAL CHEMISTRY, 1995, VOL. 14, NO. 2, 371–420

Experimental measurements of state resolved, rotationally inelastic energy transfer

by ARAM SCHIFFMAN and DAVID W. CHANDLER
Sandia National Laboratories, PO Box 969 MS 9055,
Livermore CA 94551, USA

A great deal of experimental effort has been put toward measurements of integral and differential, state-to-state cross-sections for rotationally inelastic energy transfer. Throughout the years measurements in thermal gas cells, and in crossed molecular beams, have been performed at increasingly impressive levels of quantum state detail. Because the term 'rotational energy transfer' can include collisional interchange among nuclear rotational states, magnetic sublevels, electron spin and orbital quantum levels, and vibrational angular momentum states, and can also include rotation–translation/vibration energy transfer, the field is an expansive one. In this review an array of experimental studies is encapsulated, including discussion of quantum-state propensities, their known or speculative physical origins, and the success or failure of simple energy transfer models. Discussion of progress toward the development of accurate, intermolecular potential energy surfaces, and the results of classical or quantum scattering calculations, accompanies the overview of experimental work.

1. Introduction

During the last couple of decades, a great deal of experimental innovation has gone into studies of rotational energy transfer. The motivations behind these studies are manifold, but at the root is the profound influence of rotational energy transfer in a diversity of gas phase phenomena. On the bulk level, rotationally inelastic collisions can influence viscosities [1], non-zero, second virial coefficients [1], and thermal conductivities [2]. In the chemistry of the Earth's atmosphere, rotational energy transfer competes with vibrational and electronic quenching, radiative decay, and reactive loss mechanisms in a complex interplay that determines spatial, temporal, and quantum-state distributions of many transient species [3]. Similar phenomena are at play for greenhouse gases such as CO_2 and CH_4, where absorbed infrared energy from the Earth's albedo can be collisionally transferred into rotation, thereby influencing the energy balance in the troposphere [3]. In the atmospheres of the outer planets and Titan, infrared emission from species such as CH_4 has been used to generate rotational Boltzmann plots and thereby extract local temperatures, under the assumption that sufficient collision numbers occur for rotations to thermalize within vibrationally non-equilibrium environments [4, 5]. Rotational equilibration can often be a fast and efficient process, and therefore can quench the gain of chemical lasers [6, 7]. In contrast, it has been proposed that population inversion in interstellar, OH and CH masers is created by highly state-specific, rotationally inelastic processes [8, 9]. In hydrocarbon flames, the assumption of rotation-to-translation (R–T) equilibrium is routinely invoked to infer spatial concentration maps from the measured distributions of unburned constituents [10]; knowledge of the relevant rotational energy transfer rates is essential to test such assumptions. Predissociation in electronically excited molecules can

0144–235X/95 $10·00

occur with dramatically reduced efficiency if efficient rotational, vibrational, and electronic quenching collisions are probable, as observed for S_1 formaldehyde [11]. Additionally, rotationally inelastic collisions can induce pressure broadening and line shifts in spectral transitions observed via emission [5, 12], absorption [12, 13], coherent Stokes Raman scattering (CARS) [14, 15], and four-wave mixing [16] spectroscopies.

Driven by such a multiplicity of experimental interests, there has been an ongoing need to determine the cross-sections that characterize rotational energy transfer in varied environments. Because each collision system is uniquely characterized by factors such as rotational constants, number of internal degrees of freedom, strengths of the attractive and repulsive parts of the potentials, and the possible existence of near resonant energy transfer pathways, the cross-sections for rotational energy transfer can vary greatly from one collision partner to another. This fact alone has provided the impetus for the development of many experimental methods, capable of studying increasingly broad numbers of molecular systems.

As an added layer of complexity, the cross-sections for each collision system can depend markedly on initial and final quantum state. As a simple, but dramatic, example consider the mesopheric emission from the strong OH($v'',j'' \leftarrow v' \leqslant 9, j'$) Meinel band nightglow [17, 18]. From the rotationally resolved infrared spectra, substantial population has been found from OH with as much as 33 quanta of rotation, corresponding to $\leqslant 23\,000\,\mathrm{cm}^{-1}$ of internal energy in high rovibrational states. The populations in these highly excited levels are orders of magnitude larger than predicted from extrapolation of the approximately thermal distribution of OH at low j. In explanation of such highly non-equilibrium distributions, it has been proposed that the collisional relaxation rates of OH(v,j) are near gas kinetic (i.e., hard sphere) at the lowest j levels but decrease with increasing j, falling rapidly as the energy spacings exceed kT. Similar explanations have been given for the observed, j dependent, rotational energy transfer rates in a number of systems; in many cases, the cross-sections vary with more complex, non-monotonic dependences on j and Δj. Such observations can reveal important dynamical information about rotational scattering events. The price of such knowledge, however, is a significant experimental burden: measurements of cross-sections at the *state-to-state* level of detail.

In addition to possible j-dependencies to the cross-sections, there can also be accompanying dependencies on magnetic and fine structure states. Scattering among magnetic sublevels can lead to non-equilibrium distributions in m_j, characterized by orientation, alignment, and higher moments. In polyatomic molecules, rotational energy transfer can proceed preferentially through certain k quantum numbers [19], implying preferential rotation about a particular molecular axis, or vibrational angular momentum states [20–23], implying the facile interconversion between rotational and vibrational angular momenta. Observed propensity rules for scattering among the spin states of closed or open shell, doublet or triplet species [24, 25], or among fine structure (spin–orbit and λ-doubling) states in $^2\Pi$ free radicals, can be unmistakable signatures of favourable directions for electronic spins, electronic orbital angular momenta, and orbital alignment during inelastic collisions. In addition the cross-sections may depend on the collision energy, and can exhibit glory oscillations [26, 27], energetic onsets of open channels [26], multiple encounters during a single collision ('chattering') [28, 29], and resonances on the multidimensional potential energy surface that governs the collisional interaction [26]. Clearly there are numerous experimental coordinates to be explored, generating a need for *fully* state-resolved scattering measurements.

In parallel with the growing quantity of laboratory results, there has been intense

theoretical interest in studying the factors that influence rotational energy transfer. Particular emphasis has been placed on development, tests, and refinement of empirical and *ab initio* potential energy surfaces for many simple collision systems. Comparison of observed and predicted, state-to-state, *integral* cross-sections has been an important means to evaluate the accuracy of such potentials, particularly of the anisotropies at short-range where repulsive forces dominate [30]. Furthermore, *differential* scattering cross-sections can exhibit distinctive diffraction oscillations and angular rainbow structure [27], whose amplitudes and positions are sensitive to both attractive and repulsive portions of the interaction potentials [30]. The appearances of rotational rainbows—manifested as angular maxima in the differential cross-sections, or alternatively as j-dependent peaks in the integral cross-sections—also provide unique tests of simple but powerful, classical models wherein the potentials are represented by simple repulsive forms (e.g., as rigid or 'breathing' ellipsoids). Additionally, for some collision systems several authors have modelled the j and Δj dependent cross-sections as simply parameterized, monotonically decreasing functions of energy or angular momentum gap; such *ad hoc* treatments have been useful, for example, in reproducing coherent anti-Stokes Raman scattering transition line shapes under high-pressure conditions, and predicting quenching effects in chemical laser environments. The desires to test model potentials using rigorous results of scattering theory, and to evaluate the usefulness and accuracy of approximate classical models or quantum gap scaling relations, have generated powerful motivations for laboratory studies of rotational energy transfer.

There have been several motivating experimental goals. Among them are (i) generality, or the capability to probe a broad variety of molecules, (ii) preparation of molecules in well defined, initial quantum states, (iii) collision energies that are tunable and exhibit small spreads, (iv) resolution of final scattering states, (v) capabilities for probing single-collision dynamics, (vi) high angular resolution in differential scattering measurements, (vii) measurements of *absolute* scattering cross-sections, and (viii) reasonable signal average times.

The purpose of this review is to provide a survey of collision systems that have been studied, physical understandings derived from them, and to a much lesser extent the status of related theoretical results. Since a variety of innovative experimental techniques have been employed, a subsidiary goal is to outline the methods that have been developed and employed for measurements of rotational energy transfer. Included are techniques that allow varying selectivities of initial state, final state, and range of collision energies; that are time resolved or time-integrated; and that probe either integral or differential cross-sections (or in some cases, both). The examples cited herein, while not exhaustive, are intended to be sufficiently broad in scope to convey the types of collision systems that have been investigated, and the corresponding levels of theoretical understanding. To limit the reach of this review the term 'rotational energy transfer' will denote transfer among j, m_j, spin, and orbital quantum numbers; only cursory treatment will be given to additional dependencies on vibrational state. Additionally, as the treatment of ion–molecule interactions is in itself a prodigious field, the present discussion is restricted to neutral systems.

The remainder of this review begins with a brief introduction to early methods, where j states are not resolved but which nonetheless constitute formative work for studies in subsequent years. In section 2, early experimental evidence for rotational energy transfer is briefly reviewed. Section 3 comprises a review of studies, performed in thermal gas cells, of energy transfer in electronically excited states. Descriptions of

the experimental methodologies are given. In order, the following dynamics are discussed: (3.3.) propensities and selection rules for j-changing collisions, (3.4.) propensities for m_j-changing collisions, (3.5.) the dependencies of the state-to-state, integral cross-sections on collision energy, (3.6.) energy transfer among the fine structure states in open shell, free radicals. The topic of energy transfer in the ground electronic state is taken up in section 4: (4.1.) background, (4.2.) propensities and selection rules for j- and k-changing collisions, (4.3.) energy transfer in vibrationally excited, polyatomic molecules, (4.4.) propensities for m_j-changing collisions, (4.5.) energy transfer among the fine structure states in open shell, free radicals. Section 5 covers the measurement of integral and differential cross-sections in molecular beam environments: (5.1.) background and experimental concepts, (5.2.) integral cross-sections for diatomic molecules, (5.3.) energy transfer in closed shell, polyatomic molecules, (5.4.) energy transfer among free radical fine structure states, (5.5.) measurements of differential cross-sections, with an emphasis on the development and refinement of intermolecular potentials, and (5.6.) m_j-changing collision propensities, studied at a higher level of detail. The review concludes in section 6 with a brief summary, and some indication of important, future directions.

Finally, a few words on notation are warranted. The probed molecule is called the 'target' gas, while the other collision partner will be identified either as the 'collider gas', 'buffer gas', 'bath gas', or alternatively as 'M'. The experimental quantities of interest are presented either as cross-sections or rate constants. Although rate constants are generally reported for thermal environments and when a large number of collisions occur during the observation time, while cross-sections are given when the collision velocity is more narrowly defined, the choice is nonetheless somewhat arbitrary and we follow the discretion of each author. As is customary in scattering treatments, the quantum state labels for the target gas are given in lower case. For consistency throughout this review, initial and final rotational states are denoted by j_i and j_f respectively, regardless of the notation used in the original papers. The state-to-state, integral cross-sections are $\sigma_i \rightarrow f$, the corresponding detailed rate constants are $k_i \rightarrow f$. Following the standard convention, differential cross-sections are given by $d\sigma/d\Omega$.

2. Early studies of rotational energy transfer

An excellent review of rotational energy transfer studies performed before 1980 has been given by Yardley [31]. In order to present the groundwork upon which more recent experiments have been built, we will briefly highlight some of the early work. Although rotational energy transfer, as studied today, is obviously grounded in the concept of quantum mechanical rotational levels, the early experimental evidence dates back as far as 1911, when Franck and Wood noted that visible fluorescence from I_2 could be quenched by foreign gases [32]. In ensuing decades rotational energy transfer was often studied indirectly, by its influence on bulk gas properties. For example, although the classical speed of sound for a monatomic gas is independent of frequency, this is no longer true for molecules with internal degrees of freedom. If the frequency of a sound wave and that of an internal mode in a molecule are comparable, energy can be stored in the gas and equilibrium is not maintained between translation and rotation/vibration. Thus measurements of absorption, and dispersion, of sound waves can be used to infer the efficiencies of rotational and vibrational energy transfer between degrees of freedom [33].

Other bulk measurements, from which rotational energy transfer rates have been inferred, have included measurements of the time delay between the introduction of

energy into a system and its subsequent uptake, and of the thicknesses of shock fronts [33]. From such measurements, one can estimate average relaxation rates for a collision system. Clearly, however, no information is afforded on the collision probabilities for transfer among specific rotational states. This early work set the stage for more highly detailed studies of rotationally inelastic energy transfer.

3. Thermal cell methods

3.1. *Energy transfer in electronically excited states*

In order to measure rotational energy transfer rates directly, a great variety of experiments carried out in thermal gas cells have proven to be extremely fruitful. The essence of these methods is the preparation of molecules in a non-thermal distribution of rotational levels, and monitoring of the subsequent evolution of this distribution toward equilibrium (figure 1). The initial, non-equilibrium distribution can be produced by optical pumping, flash photolytic production of a transient molecular fragment, or

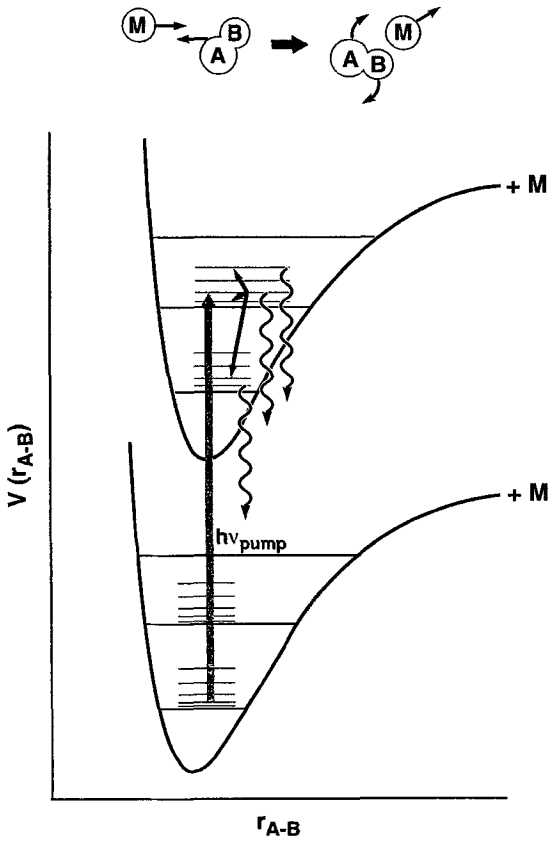

Figure 1. Schematic showing relevant processes for a typical scattering experiment of a molecule in an electronically excited state. The target molecule *AB* is optically excited to a single rovibrational v_i, j_i level of the excited electronic potential. The population is subsequently transferred to a series of final levels v_f, j_f via collisions with a collider gas *M*. The dispersed fluorescence from *AB* provides a signature of the final state populations, from which the state-to-state rate constants for rotational energy transfer may be extracted.

as the product of a chemical reaction that occurs quickly with respect to the subsequent relaxation processes of interest. Ideally a molecule would populate only a single rotational level, although frequently a number of states are initially formed. The population of the target molecule in a given quantum state is then monitored optically, in a manner that resolves individual rotational states (e.g., dispersed fluorescence), as relaxation occurs through collisions with a thermal bath of collider gas. Such methods date back to the 1959 study of Carrington [34], who used Bi resonance emission to excite OH ($A^2\Sigma^+$, $v = 0, j = 10{\cdot}5$) in an acetylene–O_2 flame and observed a mildly relaxed j_f distribution from the dispersed fluorescence spectrum. In general, by varying the pressure of M and thus varying the collision number for a fixed time interval, the state-to-state rates for rotational energy transfer can be inferred from the j-dependent signals. Note that the resulting rates are inherently averaged over Boltzmann distributions of collision velocities and, for molecular collider gases, of internal states.

3.2. *Experimental considerations*

The earliest techniques for preparing a target gas in an initially excited state took advantage of coincidences between molecular absorption features and the emission frequencies of common atomic resonance lamp lines. The gas cell is subjected to continuous illumination at the resonant frequency, which pumps a fraction of the target molecules into an electronically and rotationally excited (j_i) level; the ensuing transfer of population in the excited states is monitored as a function of j using dispersed fluorescence. If j-changing collisions occur within the radiative lifetime of the excited molecule, fluorescence is observed not only from the so called 'parent' line originating from j_i, but also from 'satellite' transitions originating from $j_f \neq j_i$. If the j-dependent transition strengths are known, the emission spectrum can be used to retrieve the relative populations in j_i and all observed j_f. With sufficient detection sensitivity the experiments may be performed at low pressures, such that single collision conditions dominate on the time-scale of emission. The goal is then to determine the state-to-state rate constants from the rotationally resolved signal strengths.

Commonly, at least two difficulties can impede such analysis. First, the pump light may only partially overlap the molecular transition within a pressure- and Doppler-broadened line-width. As the lamp conditions vary the extent of this overlap may change with time, interfering with the reproducibility of the measurements. This difficulty has largely been overcome with the use of c.w. lasers as alternative sources of pump light. In early studies, ion lasers have been employed for their stable and well-calibrated lasing frequencies, again requiring their accidental overlap with molecular transitions. The advent of *tunable*, spectrally narrow dye lasers has dramatically increased the number of molecular species that may be optically pumped, as well as the number of quantum levels in which they may prepared.

Second, one would like to approach the limit in which each j_f is populated in a single collision, so that the observed populations directly reflect the state-to-state cross-sections. Unfortunately, the effects of multiple collisions can never be totally eliminated. The probability P_n that a molecule has undergone n collisions is given by the Poisson distribution:

$$P_n = \mu^n e^{-\mu}/n!, \tag{1}$$

where μ is the collision probability. As an example, a 50% collision probability (i.e. $\mu = 0{\cdot}5$) implies that almost 10% (more precisely, 0·08) of the molecules have

collided twice. Even when the single collision probability is reduced to 10% (i.e., $\mu \sim 0{\cdot}11$), about 0·6% of all molecules have experienced multiple collisions, or $\sim 1/20$ of the number that have had one collision. As a consequence of this somewhat unforgiving function, the influences of multiple collisions must be modelled even for quite low gas pressures where energy transfer is relatively inefficient. Such analysis tends to introduce the largest errors on the most weakly populated states, generally with large Δj, where higher-order collision processes have the largest effects. Still, at low cell pressures these influences can be made arbitrarily small, given sufficient detection sensitivity. The influences of multiple collisions can also be probed quite directly, and largely eliminated by lowering the cell pressure until the emission intensities vary linearly with buffer gas concentration.

3.3. j-*changing collisions*

Conceptually, the simplest rotational energy transfer event is a change in the nuclear rotation, that is, a j-changing collision. In a remarkable early study, Broida and Carrington took advantage of the strong and narrow band emission line at 2144 Å from Cd II, to prepare NO ($^2\Sigma^+$, $v = 1, j_i = 12{\cdot}5, 13{\cdot}5$) in a quartz cell [35]. In the presence of $\leqslant 3$ Torr of NO ($X^2\Pi$), He, Ar, H_2, N_2, or CO_2, fluorescence was observed and dispersed from $v' = 0, 1$ and a large number of j_f. Through extensive calibrations of the Cd lamp emission lineshape, the NO ($^2\Sigma^+$) emission strengths, fluorescence line-widths, and electronic quenching rates the authors extracted the relative populations of NO in each j_f based on the emission line strengths. In an effort to model the observed rotational population distributions as a function of buffer gas pressure, the authors applied successive kinetic models that allowed increasingly large Δj to occur. It was found that by assuming the simplest selection rule $|\Delta j| = \pm 1$, the data could not be well reproduced; in fact the best fit to the data was found with an energy transfer probability density function extending to multiple rotational quanta. Collisions were found to be important with up to five quanta gained or lost, demonstrating the importance of multiquantum jumps in the rotational energy transfer process. Similarly large quantum jumps are operative in other collision systems. Steinfeld and Klemperer have investigated rotational energy transfer in $I_2(B^3\Pi_{ou+}, v' = 25, j' = 34) + {}^3He, {}^4He$, Ne, Ar, Kr, Xe, H_2, O_2, CO_2, SO_2, CH_3Cl, and NH_3 [36]. Dispersed fluorescence was obtained from rotational transitions in several Franck–Condon bands with $v' = 24$–27. Only transitions with $\Delta j = 0, 2, 4, \ldots$ were observed, i.e., transitions that preserve the total (rotational + nuclear spin) symmetry, confirming the expected result that collisions are extraordinarily unlikely to flip an atom nuclear spin and thus permit odd Δj quantum changes. Notably, transitions with Δj as large as 20 were observed even at the lowest cell pressures where multiple collisions are minimized, again emphasizing the importance of large quantum changes.

In some cases, the state-to-state cross-sections can exhibit a remarkably simple dependence on j and Δj. Brunner *et al.* have used a c.w. dye laser to pump $Na_2(A^1\Sigma_u^+)$ into levels with j_i ranging from 4 to 100 [37–40], in the presence of He, Ne, Ar, Kr, Xe, H_2, N_2 or CH_4 buffer gas. The resonance fluorescence was dispersed in a double monochromator set to view the emission from the parent and a satellite line simultaneously, and corrected for saturation, background signals, and the estimated effects of multiple collisions. The total loss rate constants were found to decrease monotonically with increasing j_i, a qualitative trend also observed in several studies of hydrogen halides in their ground electronic states (see below). As j increases, the decline in $k_i \rightarrow_f$ is generally attributed to an increasing energy spacing between rotational levels,

and the correspondingly smaller fraction of the translational Boltzmann distribution with sufficient collision energy to induce a change in j. Such reasoning has led to the development of energy-gap-based scaling relations for the state-to-state cross-sections. As will be shown for a number of cases throughout this review, however, the j-dependence to the state-to-state cross-sections can be considerably more complex, and it is generally not a *priori* obvious when such energy gap formulations should be reliable. For example, when NaK + He is investigated [41, 42], j changing collisions are found to be inefficient for $j_i \leqslant 30$, but are more probable for higher initial rotational states, a result for which no clear explanation is evident.

The cross-sections for a given target gas also show some interesting dependencies on the identity of the collider gas. Caughey and Crosley [43] have used a Zn lamp to excite $S_2(B^3\Sigma_u^-, v' = 4, n_i = 40, j_i = 41)$, in a heated cell (630°C) containing up to ~ 20 Torr of H_2, N_2, He, Ne, Ar, Kr, or Xe. Here n is the quantum number for end-over-end tumbling of the nuclei, while j is the total angular momentum including spin. Because the satellite lines are largely overlapped in the dispersed fluorescence spectrum, the rotational band contours were modelled as a function of collider gas pressure, and the relaxation rated modelled in the steady state approximation for the population in each vibrational level. It was determined that the average change in j per collision increases with increasing collider gas mass. For the rare gases, a monotonic increase is observed in the relative cross-sections for total relaxation out of the initial ($j = 41$) state, as the collision reduced mass μ is increased in the series He, Ne, Ar, Kr; the corresponding cross-section for Xe, however, is smaller than that for Kr and is roughly equal to that for Ar. The reduced mass is related to the scalar, orbital angular momentum, L, in a collision with impact parameter b via

$$L = \mu v_{\text{coll}} b = (2E_{\text{coll}}\mu)^{1/2} b, \tag{2}$$

where v_{coll} and E_{coll} are the centre of mass collision velocity and energy, respectively. Since L scales as $\mu^{1/2}$ the authors propose that the rising trend may simply reflect a steadily increasing reserve of available angular momentum, although this argument apparently does not extrapolate to Xe. Similar increases in $k_{i \to f}$ with collider gas mass have been observed by Steinfeld and Klemperer [36] for I_2 + rare gases in their fully state-resolved studies, and Brunner *et al.* for $Na_2(A^1\Sigma_u^+, j \leqslant 100)$ + He, Ne, Ar, Kr, and Xe. As will be noted below, this interpretation must be slightly amended for very rapidly rotating molecules, such as hydrogen halides in high j states, where rotational averaging of the potential can become important. Nonetheless, for diatomic rotors and rare gases, simply invoking such a simple angular momentum constraint can account qualitatively for a majority of the observed mass-dependent rate constants.

For *molecular* buffer gases, several new factors become important. Internal modes of the collider can serve as repositories for excess energy, opening up the possibility of near-resonant exchange of rotational quanta with a concomitant enhancement of the rotational energy transfer rates. Notable examples have been found in Caughey and Crosley's studies of $S_2 + M$ [43], in which the cross-sections for H_2 and N_2 are larger than those for He and Ar respectively, despite slightly smaller reduced masses in each case. Brunner *et al.* [40] have noted a $\sim 25\%$ increase in the total rate of energy transfer out of $Na_2(A^1\Sigma_u^+, j_i = 16) + CH_4$ against Ne, again despite the slightly smaller reduced mass for the former. From Broida and Carrington's data on NO + He, Ar, H_2, N_2, or CO_2 [35] the rate constants are found to be near gas-kinetic, implying large cross-sections (tens of $Å^2$) for all M, but with the highest efficiencies nonetheless occurring for the diatomic collision partners. Moreover Steinfeld and Klemperer [36]

have found that for $I_2(B^3\Pi_{ou+}, v' = 25, j_i = 34) + M$, the rotationally inelastic cross-sections generally increase with increasing collision reduced mass, but with $\leqslant 2$ fold larger cross-sections for the *polar* molecules CO_2, SO_2,and CH_3Cl than for the non-polar species with corresponding masses. This suggests that long-range, attractive forces can significantly influence the transfer of rotational motion, in effect adding a tail at long intermolecular distances to the opacity function for rotational energy transfer.

When rotational energy transfer is accompanied by a change in vibrational state, the dynamics can change considerably. In the $I_2(B^3\Pi_{ou+}) + M$ studies of Steinfeld and Klemperer mentioned above [36], fluorescence was observed not only from the nascent $v_i = 25$ vibrational levels, but also more weakly from states with $\Delta v = \pm 1, \pm 2$. While emission from $v = 25$ is quite strongly peaked around the initially selected, $j_i = 34$ rotational level, the rotational distributions become increasingly broad with changes in vibrational state in the order $\Delta v = 0, -1, +1, -2, +2$. This effect is most pronounced for more massive collider gases. A similar phenomenon appears in the studies of $S_2(B^1\Sigma_u, v' = 4) + M$ by Caughey and Crosley [43], where it was observed that as population decays through *vibrational* levels with $v < 4$, the overall *rotational* contours are largely relaxed, exhibiting little excess population in j states close to the initially excited rotational level. As pointed out by Steinfeld and Klemperer, the characteristically large changes in j that apparently accompany a change in vibrational state can be readily rationalized. Simple Landau–Teller theory predicts that vibrational energy transfer is most efficient for highly impulsive collisions, which in turn are liable to have sufficient force to cause large changes in j. Presumably, collisions either with small impact parameter (most likely end-on collisions) or in the high-energy wing of the Boltzmann speed distribution cause vibrations to change; such collisions are also most likely to cause a large change in rotational quantum number as well. Since the average collision velocity decreases with increasing collider gas mass, then for heavier M the vibrational energy transfer probability is reduced and a more selective subset of possible trajectories lead to the final distribution.

In summary, these early studies, along with many not mentioned here, have shown that rotational energy transfer of diatomic molecules, measured in electronically excited states, can proceed with quite large changes of rotational quanta. For molecules that are not rotating rapidly with respect to the collision duration, the energy transfer cross-sections tend to increase with increasing collider gas mass, due to the increased availability of orbital angular momentum. Near resonant rotation–rotation energy transfer with molecular collision partners can distinctly increase the collision cross-sections; long-range interactions with dipolar molecules can provide a further enhancement.

3.4. m_j-*changing collisions*

Through clever choice of pump laser polarization, measurements can also be made of m_j-changing collision rates. This possibility arises because a one-photon, electric dipole transition moment can depend quite dramatically on the initial and final, magnetic quantum numbers; if a P or R branch line is pumped with circularly polarized light, a non-uniform distribution of m_j levels will be prepared in the excited state (figure 2). For example, the R branch transition moments for a rigid rotor with zero nuclear spin, and no curve crossings present in the electronically excited state, are (suppressing Franck–Condon factors) [44]

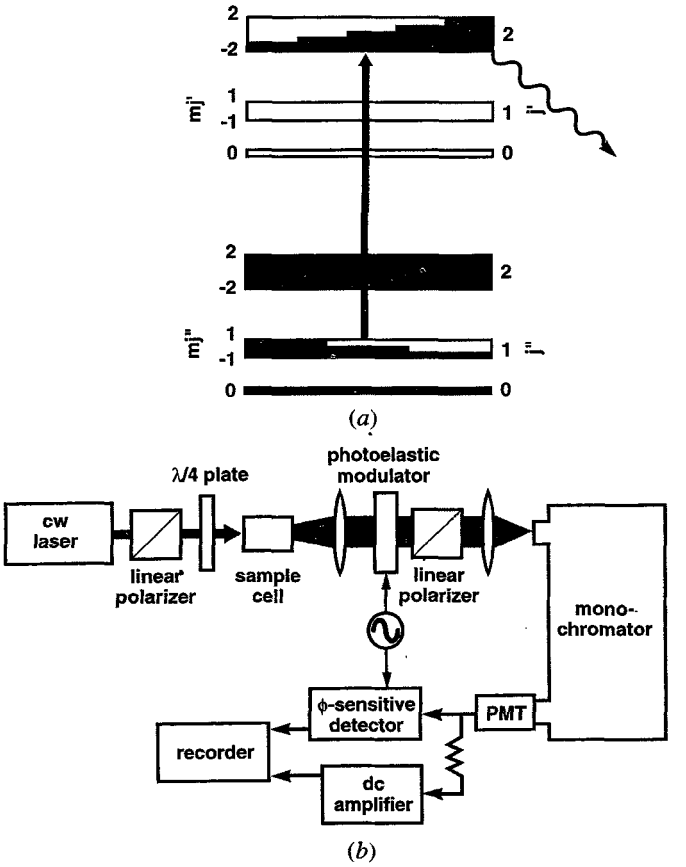

Figure 2. (*a*) Preparation of a non-uniform distribution in m_j, for a hypothetical molecule, by optical pumping with circularly polarized laser light. The retention or loss of circular polarization, in the emission from the excited state, reflects the degree of collisional redistribution among the m_j states. (Adapted from [45]). (*b*) Experimental apparatus for determination of the circular polarization of fluorescence from an optically prepared sample. (Adapted from [44]).

$$\left.\begin{aligned}\langle j''m_j''|E_+|j'+1m_j''+1\rangle &\propto \left[\frac{(j''-m_j''+1)(j''-m_j''+2)}{2(2j''+1)(2j''+3)}\right]^{1/2},\\ \langle j''m_j''|E_-|j'+1m_j''-1\rangle &\propto \left[\frac{(j''-m_j''+2)(j''-m_j''+1)}{2(2j''+1)(2j''+3)}\right]^{1/2},\end{aligned}\right\} \tag{3}$$

where single and double primes label excited and ground states respectively, and $E_\pm$ are the circular components of the radiation electric field vector that rotate counter-clockwise/clockwise as the light propagates away from the observer. From the line strengths in equation (3), it can be seen that a distribution of states will be produced with increasing population with increasing (or decreasing) m_j' depending on the choice of circular polarization.

The subsequent emission from the parent or satellite lines of the electronically excited state is thus also polarized, until sufficient collisions have occurred to randomize the population in the magnetic sublevels. If this randomization is slow with respect to

the j-changing collision rates, then the emission is eliptically polarized with components E_+ and E_- that are readily calculated as a function of j [44]. The emitted light can be characterized by a ratio C:

$$C = \frac{I_+ - I_-}{I_+ + I_-}, \tag{4}$$

where $I_\pm$ are the intensities of the two light polarizations. The signs and magnitudes of the j-dependent C values directly probe the extent to which the emitted light is depolarized, and hence the extent to which m_j-changing collisions have occurred [44]. Note that this technique is based on j- and m_j-dependent transition moments for photon absorption and emission, rather than explicit spectral resolution of the m_j states, and thus can be applied to transitions with arbitrarily broad Doppler widths.

The group of McCaffery has used such an arrangement extensively, initially for studies of rotational energy transfer in I_2 + Ar, O_2, and I_2 [45]. One or several j states in $I_2^*(^3\Pi_{ou+})$ were pumped simultaneously with circularly polarized light from an Ar^+ laser, or alternatively with a tunable, narrow band, c.w. dye laser. For all collider gases and for each j investigated, C is essentially unchanged as a function of cell pressure up to several hundred Torr. Remarkably, this observation implies an m_j distribution that is largely undisturbed over many gas kinetic collisions, even under conditions where substantial, collision-induced population of $j_f = j_i \pm 0, 2, 4, 6 \ldots$ is observed.

To investigate the possibility that a molecule with a different mass and rotor constant might behave differently, McCaffery and coworkers have extended these studies to $Li_2(^1\Sigma_g)$ + He, Ar. Here, several levels were pumped with a circularly polarized, multimode Ar^+ laser; the resulting parent and satellite emission was similarly analysed for + and − polarization intensities. For rotationally elastic collisions (i.e., $j_i = j_f$), the circular polarization ratio C was observed to be essentially constant up to ~ 100 Torr of collider gas pressure, corresponding to an average of more than ten gas kinetic collisions per excited state lifetime. The depolarization ratio is similarly constant for inelastic ($j_i \neq j_f$) collisions with He; in the case of Ar a mild dependence of C as a function of collider gas pressure was found, indicating slightly more facile interconversion among the magnetic sublevels. In further studies, Whitaker and McCaffery have investigated rotational energy transfer in the potentially reactive NH_2 + H, where the system NH_2 was generated in a flow cell via the reaction of hydrazine. In this system a substantial, though unquantified, degree of m_j reorientation was observed, with a dependence on the rotational and spin states. Reorientation of j, during an inelastic collision of a polyatomic molecule, appears to be a more facile process than in diatomic species.

The physical origins of the persistence of non-equilibrium m_j distributions against large collision numbers, at least for the diatomic species investigated, have been investigated theoretically by Jeyes *et al.* [46] In these studies, the authors calculated the j-dependent values of C that would be observed presupposing either of two hypothetical constraints on Δm_j. In the first, it is assumed that m_j is unchanged in a collision. In the second, the classical orientation angle θ of the angular momentum vector is presumed to be unaltered, where θ is given by

$$\theta = \cos^{-1}\left[\frac{m_{j_i}}{j_i(j_i+1)}\right]^{1/2}. \tag{5}$$

Comparison of predicted and observed depolarization ratios shows that the latter model, in which the classical precession angle remains constant, is decidedly inconsistent with

the observed values of C. On the other hand, impressive agreement is found for the former (m_j-preserving) model over a wide range of j_f. These results suggest a very strong propensity for small changes in m_j. These data afford compelling evidence that the distribution of magnetic sublevels in these diatomic molecules is not readily disturbed by collisions. An implied result is that if Δj is large and $m_{j_i} \sim j_i$ then the angle θ can change considerably (5). In other words, according to this interpretation the molecule must undergo surprisingly large changes in its tilt angle during rotationally inelastic collisions. We note that a different interpretation, whereby θ is strongly conserved in the collision, has since been proposed based on scattering of N_2 in the ground electronic states; this topic is taken up in section 4.3.

3.5. *Velocity dependence of collision cross-sections*

The use of a tunable dye laser as the pump source can provide, in addition to wide j_i selectability, a convenient way to select the collision *velocities* by means of the Doppler shift and therefore to study the influence of collision energy on the state-to-state rate constants. Specifically, in order to project onto the laser axis at a given Doppler shift $\Delta\nu$, a target gas molecule must have a minimum speed $v_{\min}$ given by

$$v_{\min} = c\left(1 + \frac{\Delta\upsilon}{\nu_0}\right), \tag{6}$$

where ν_0 is the frequency at line centre and c is the speed of light. For a given $\Delta\nu$, molecules whose speeds v are in the range of $0 < v < v_{\min}$ remain unexcited by the pump laser, skewing the excited target gas translational distribution to increasingly high velocities with increasing absolute value of the Doppler detuning. If rotational energy transfer occurs before the translational distribution can relax, then the resulting emission spectrum provides a measure of the velocity-dependent, state-to-state rate constants.

Smith, Brunner and Pritchard [47, 48] have used a tunable, c.w. dye laser to pump a given v_i, j_i in $Na_2(A^1\Sigma_u^+)$ in the presence of excess Xe ($\leqslant 1{\cdot}2$ Torr); the authors give useful expressions for the velocity distribution prepared in the excited state of the target gas as a function of Doppler shift. The emission from a parent line with $j_i = 16$, 38, or 66 was monitored, and the energy dependence of the rate constants $k_{i\to f}$ obtained from the relative parent/satellite intensities by integrating over the nascent velocity distributions (figure 3). For all collisions with $j_i = 38$ the rate constants were found to increase roughly linearly with increasing collision velocity. When $j_i = 16$ is prepared, for small Δj ($\leqslant +10$) the rate constants $k_{i\to f}$ increase with velocity but exhibit a distinct *downward* curvature that is increasingly pronounced with increasing change in j. For $\Delta j = +16$ (the largest value reported) $k_{i\to f}$ reaches a maximum, followed by a steady decline, at around twice the mean thermal velocity. The authors hypothesize that only short-range collisions can sample an adequately anisotropic portion of the potential to induce large, fractional changes in j; because of long-range attractive forces, slower atoms are most likely to be drawn in close. However, it is also noted that for $j_i = 66$ the rate constants $k_{i\to f}$ exhibit *upward* curvature as a function of velocity, for Δj as large as $+6$, an observation the authors attribute to a competing effect: the increasingly angle-averaged potential that a slow-moving Xe sees due to the rapidly rotating Na_2

3.6. *Energy transfer between spin–orbit states and λ-doublets*

When a molecule is prepared in a $^1\Pi$ electronic state, the unit of orbital angular momentum serves as a potential vehicle for the transfer of angular momentum, whose

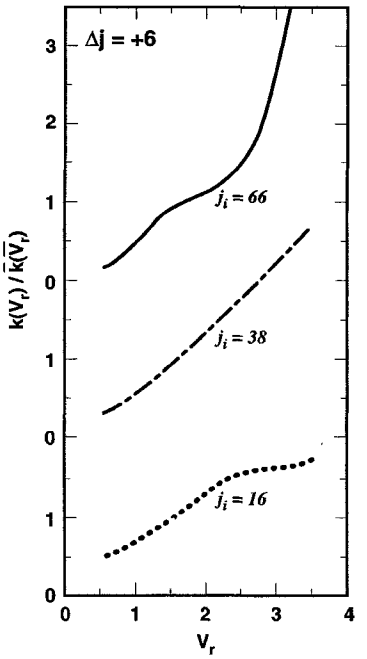

Figure 3. Dependence of the state-to-state rate constants for Na_2 + Xe ([48]) on the velocity, as a function of j_i and Δj. The x-axis label v_r is the speed normalized to the mean thermal value. At high rotational levels (e.g., $j_i = 66$, lower curve) the rate constants rise with increasing velocity, due to an increase of available orbital angular momentum. This may also be explained by a reduction in the rotational averaging of the potential as the collision duration becomes increasingly short. For low rotational levels (e.g., $j_i = 16$) and large Δj, a maximum is observed in the rate constant as a function of velocity, suggesting that slower speeds are more favourable and consistent with complex formation in the energy transfer process.

physical significance is as follows [49]. In a non-rotating molecule, the two states with orbital angular momentum projections $\lambda = \pm 1$ are degenerate. When the nuclei are tumbling, however, this degeneracy is lifted, and two 'λ-doublet' states are formed for each rotational level (Quantum mechanically, the splitting between the λ-doublet states arises from perturbations due to a nearby Σ state, which lowers the energy of one level but not the other). In the high j limit, these two states differ in that the lobes of the excited electronic orbital lie in the plane or out of the plane of nuclear rotation. Since collisional interconversion of the λ-doublet levels implies a reorientation of this singly occupied orbital, an event that presumably requires a rather specific type of collision trajectory, the *e/f* dependence of the rotational energy transfer rates can illuminate the underlying collision mechanisms. An important experimental point is that the two λ-doublet states, although typically split by very small energies (fractions of a cm^{-1}), radiate in separate branches in a $^1\Sigma \leftarrow {}^1\Pi$ emission spectrum, and therefore can be readily resolved.

As early as 1969, Zare and coworkers [50] used light from c.w. Ar^+ ion laser to excite two isotropic variations of lithium, $^7Li_2$ or $^6Li^7Li$, ($B^1\Pi_u$, $v, j_i = 9, 24, 30, 31, 38, 45, 61$) vapour, in the presence of 0·15–15 Torr of Ar buffer gas. The final state distributions, populated through rotational energy transfer in the electronically excited $B^1\Pi_u$ state, were probed via satellite transitions in the fluorescence spectrum. For $^7Li_2$, collision-induced transitions were observed with $\Delta j = \pm 1, \pm 2$; note that without the

unit of orbital angular momentum in the Π electronic state, $\Delta j = 1$ transitions would be forbidden by symmetry as mentioned above I_2. Only transitions which preserve the initial *s* or *a* electronic wavefunction symmetry were observed, as rigorously required for a homonuclear diatomic molecule in a Π electronic state. For the heteronuclear species $^6Li^7Li$, were the nuclear wavefunction symmetry is broken, additional but weak transitions were observed with $s \leftrightarrow a$. For either molecule and all j_i, collisions that preserve the λ-doublet character result in equally probable $\pm \Delta j$ jumps (for $|\Delta j| = 1, 2,$ or 3). In contrast, when a collision induces a change $e \rightarrow f$, a larger propensity is observed for a given $+\Delta j$ quantum change than for the corresponding $-\Delta j$, an ordering that is reversed for $f \rightarrow e$.

Lemoine *et al.* [51] have investigated theoretically the origin of the asymmetry in the up/down Δj cross-sections, and accompanying dependencies on initial and final λ-doublet states. The authors have pointed out that the essential concept is the existence of two intermolecular potential energy surfaces, A' and A'', distinguished by the orientation of the unpaired electron orbital. Because both of these surfaces govern the collision dynamics, quantum interferences in the scattering process can occur, resulting in the unusual Δj and λ-doublet selectively. As model systems, scattering calculations were carried out for $Li_2(B^1\Pi_u)$ + He and Ne. It was found that the ratio for up/down Δj transitions alternates between > 1 and < 1 for odd Δj, while no such alternation is observed when Δj is even. The phase and contrast of these oscillations are quite sensitive to the anistropies of the two potentials, suggesting that state-resolved cross-sections for λ-doublet changing collisions might be useful in empirical evaluation of theoretical potential energy surfaces. In any event, these interferences effects are clearly not reliably predicted by classical models for the energy transfer process. As will be seen below, similar interpretations have been given for spin–orbit state-specific energy transfer in $^2\Pi$ molecules, again in terms of scattering interferences on the A' and A'' surfaces.

Qualitatively different correlations between *j*-changing and λ-doublet changing collisions can occur in different collision systems, as has been observed in later studies by McCaffery and coworkers of NaK and Na_2 + He, Ne, Ar, Kr, Xe, N_2, H_2, and CO_2 [41, 42]. Here the ratio of rates for $\Delta j = +1$: $\Delta j = -1$ was found to increase with increasing pressure of certain collision partners (Xe, Kr, and H_2 for Na_2, and Ar, Kr, and Xe for NaK) for unexplained reasons [52]. Furthermore, as the pressure of any of these same collider gases was raised ($\leqslant 90$ mTorr), a concomitant increase was observed in the rate of λ-doublet changing collisions when the *e* but not the *f* component was prepared. These phenomena appear to occur only if the collision duration is long with respect to the rotational period, or if the attractive minimum in the interaction potential is greater than the mean collision energy. Coupled with the observation that the magnitudes of the effects were enhanced with decreasing cell temperature and hence decreasing collision energy, it was postulated that long-lived collision complexes are formed in these systems. Since the enhancement in energy transfer rates is observed only for *e* states, in which the unpaired electron lies in the plane of rotation (in the high *j* limit), the authors suggest that tee-shaped structure might be formed with the atom nestled between the lobes of this orbital. In any case, the evidence strongly supports complex formation, which in turn can have a remarkable and highly selective influence on the energy transfer rates.

While the studies discussed thus far are predominantly limited to closed shell species, there has been long-standing, related interest in energy transfer among *open shell* radicals, due largely to their influence in atmospheric and flame chemistries.

Of all open shell species the OH radical has been of particularly renowned importance, due largely to its activity as an atmospheric reagent and infrared emitter [3], and to its ubiquity in flames [53]. A principal, experimental challenge is the preparation of such a highly reactive, transient species. Lengel and Crosley [54] have carried out studies of rotational energy transfer in $OH(A^2\Sigma^+) + Ar$, H_2, and N_2 in which ground state $OH(X^2\Pi)$ was first prepared in a vacuum chamber from the gas kinetic reaction of H atoms, formed in a microwave discharge, with NO_2 [54]. $OH(A^2\Sigma^+, v = 0, n_i = 0, 1, 3, 4, 6)$ was then pumped with pulsed light from a frequency doubled dye laser, and allowed to interact with a low pressure background of collider gas. For each gas, a state-to-state rate constant matrix was fitted to the n_f-dependent populations, as determined from the line strengths of the resulting dispersed emission spectrum under steady state assumptions. For all gases a monotonic fall-off was observed in $k_{i\to f}$ against Δn, in qualitative accordance with simple energy gap scaling predictions. A propensity was observed for conservation of spin during collisions, i.e., a larger rate constant for transitions which preserve rather than alter the electronic spin state. Furthermore, the total loss rate constant (i.e., summed over all n_f) is roughly independent of the initial rotational state that is excited. Interestingly, a given $k_{i\to f}$ is larger for the structureless Ar atom than for H_2 despite the availability of rotation–rotation (R–R) energy transfer for the latter. This observation probably arises because very few rotational relaxation channels ($\leqslant 5$) are open at the collision energies studied, and the light mass of the H_2 renders it inefficient at rotational energy transfer. The corresponding cross-sections for $M = N_2$ are somewhat larger than those for Ar, possibly reflecting the availability of R–R pathways.

It is known from extensive studies of the Ar–OH van der Waals complex [55–59] that the attractive well depth increases from $\sim 100\,cm^{-1}$ in the ground state ($X^2\Pi$) to $\sim 1100\,cm^{-1}$ in the electronically excited state ($A^2\Sigma^+$). Therefore, at thermal collision energies one would anticipate quite distinct collision dynamics upon electronic excitation. Jorg *et al.* [60] have used pulsed, laser induced fluorescence to investigate rotational energy transfer in $OH(A^2\Sigma^+) + He$, Ar. Qualitatively, different sets of propensities were observed for the two rare gases. For Ar, energy transfer is enhanced among nearly isoenergetic states with $\Delta j = 1$, $\Delta n = 0$. Somewhat surprisingly this implies that the orientation, but not the magnitude, of the nuclear rotation is most likely to be altered in a collision. In contrast, collisions with He are somewhat more likely to produce transitions with $\Delta j = \Delta n = 2$. In other words, the direction of the nuclear rotation is not readily changed. These propensities are also seen in the theoretical scattering calculations of Degli Esposti *et al.* [61] for OH + Ar, and Jorg *et al.* [62]. The *ab initio* potential energy surface for $OH(A^2\Sigma^+) + He$ is dominated by even terms in an expansion in Legendre polynomials, resulting in the observed propensity for even Δj transitions. Furthermore, the potential is only weakly attractive, with a maximum well depth of $107\,cm^{-1}$ at the linear He–OH geometry; consequently, collisions are not strong and are unlikely to reorient the direction of nuclear rotation. On the other hand, the well in the $OH(A^2\Sigma) + Ar$ potential ($\sim 1100\text{-}cm^{-1}$) is rather deep with respect to mean, thermal collision energies. It is likely that energy transfer can proceed through an OH + Ar complex, which may explain the different behaviour for Ar compared with He.

Dufour *et al.* [63] have used a tunable, c.w. dye laser to excite low j levels in a particular spin–orbit and λ-doublet state of $CaF(A^2\Pi, v_i = 0)$; the fluorescence was dispersed in a 1·5 m grating spectrometer [63]. From the relative emission intensities taken at several cell pressures (0·25–2 Torr), a strong propensity was observed for

collisions to preserve the *e/f* label, an effect that becomes more pronounced at higher j_i. Moreover, the cross-sections for collisions that *conserve* the *e/f* label are larger for the $\Omega = 1/2$ spin–orbit state than for $\Omega = 3/2$, an ordering that is reversed for collisions that *change* the *e/f* label. Relative cross-sections calculated in the infinite-order sudden approximation, in which the collision time is assumed to be fast with respect to a rotor period, and the fractional energy loss per collision assumed to be small, generally agree well with the experimental cross-section values for CaF + Ar collisions. Given the high mean speed of the light He projectile, it might be anticipated that the sudden approximation is even more accurate for CaF + He. Somewhat surprisingly, however, similar calculations fail to predict the large difference between the cross-sections in the two spin–orbit manifolds. The physical origin of this discrepancy is not clear.

To summarize briefly, in an impulsive collision, strong correlations between j-changing and λ-doublet-changing collisions can arise from interferences on the A'' and A' potential energy surfaces. The formation of collision complexes can enhance the interconversion of spin–orbit, and of λ-doublet, levels. Consequently, the likelihood that these fine structure levels are preserved or changed can depend on the ambient temperature, the masses of the colliders, and the strength of the attractive portion of the interaction potential. The possibility of preferential, state-selective, collisional preparation of one fine structure level has important implications in the formation of interstellar masers, as discussed below.

4. Energy transfer in ground electronic states: thermal cell methods

4.1. *Background*

Although visible/ultraviolet laser-based pump techniques have been employed with formidable success in rotational energy transfer studies, these methods are nonetheless found wanting in several respects. For example, these techniques predominantly monitor energy transfer in *excited* electronic states, yet often it is the *ground* state's rates that are of the most direct relevance to atmospheric chemistry, combustion chemistry, interstellar maser action, and operation of chemical lasers. Additionally, many molecules predissociate rapidly in their lowest excited electronic states, and thus emit with extremely low quantum efficiency [64], effectively precluding fluorescence detection. The use of microwave and infrared radiation, on the other hand, can be used to excite or probe most molecular species while the molecules remain on their ground electronic potentials.

4.2. j- *and* k- *changing collisions*

Microwave–microwave double resonance experiments were among the first techniques used to measure ground electronic state rotational energy transfer rates. With these methods, developed by Oka [65], intense microwave radiation from a 'pump' klystron is used to saturate a rotational transition, thus disturbing the nascent Boltzmann distribution. The population differences between various rotational states are probed with a second, weaker microwave source (the 'signal' radiation); collision induced population transfer is manifested by changes in the steady-state absorption with the pump source on against off. Oka has used such a scheme for measurements of energy transfer in the symmetric top NH_3 in a bath of NH_3, He, Ar, or Xe [19]. Oka found that when NH_3 is both target and collider [19], energy transfer is largely restricted to $\Delta j = 0, \pm 1$, with a strong propensity for parity changing collisions, $+ \leftrightarrow -$. The parity label refers to reflection of the rotation-inversion wavefunction through a plane

perpendicular to the symmetry axis. This is precisely the selectively that is anticipated if long-range, dipole–dipole forces dominate the collisional interaction. In addition, a propensity for $\Delta k = 0$ is observed, i.e., no change in rotation about the symmetry axis. For levels with $j \sim k$, transitions with $\Delta j = 0$ are stronger than those with $\Delta j = \pm 1$, whereas the rates are similar when $j \gg k$.

For NH_3 + He, Ar, and Xe, dipole–dipole interactions are no longer present and higher-order, electrostatic moments determine the shape and strength of the intermolecular potential. Thus one anticipates quite different selectivity for collisional energy transfer among j and parity levels than is observed for NH_3 self-relaxation. Such expectations are indeed borne out. As one striking difference, collision induced transitions are inferred with $|\Delta j| \leqslant 6$, with no simple constraints on the magnitude of the cross-sections as a function of Δj. Additionally, the + and − parity levels appear to interconvert freely, in contrast to the $+ \leftrightarrow -$ propensity observed in pure NH_3. On the other hand, changes in the quantum number k are strongly limited to integral multiples of three. In explanation Oka has demonstrated that in an expansion of the potential in electrostatic moments, the lowest term with the proper symmetry to change k is a component of the octopole-moment tensor. For pure rotational energy transfer, the octopole (NH_3)–dipole-induced-dipole (rare gas) interaction drives the $\Delta k = 3$ transitions. Other changes in k follow from higher, and presumably weaker, terms in the series. Taken collectively, these observations imply that rotational energy transfer in NH_3 + rare gases occurs via strong, fairly short-range collisions.

One experimental complication of such a double-resonance technique, with two continuous wave sources of radiation, is the possibility that the measured populations reflect the product of multiple collisions. In order to discriminate against such sequential quantum changes, an inherently short time-scale can be introduced by modulating pump intensity on and off with a square wave ($\omega \sim 100$ kHz), and phase-sensitively detecting the absorption signal at ω [66]. The resulting signal amplitudes and phase shifts reflect dynamics on a microsecond timescale, which under low pressure conditions (tens of mTorr) can readily sample the single collision regime. Gordon *et al.* [66] have used such a technique to measure rotational energy transfer in HCN, optically excited to $j_i = 10$ in $v = 1$ of the doubly degenerate bend, and transferred to $j_f = 11$, 12, 13 via collisions with HCN. The rate constants for energy transfer among these states, fitted under constraints of detailed balance, indicate that $\Delta j = 2$ transitions are only ~fourfold less important than those with $\Delta j = 1$, and that $\Delta j = 3$ transitions contribute substantially as well. For HCN + Ar transitions with $\Delta j = +2$, a strong propensity is observed to preserve the parity of the HCN 1-doublets during the collision. The observed cross-sections are quite small, indicating that the collisional interactions are predominately short-range, sampling the repulsive wall of the potential at small r. From the observed propensity rules, the authors argue that even at close range the interaction potentials are highly anisotropic.

The development of infrared, chemical lasers has generated specific interest in infrared based methods; of great pragmatic importance is the possibility that rotational thermalization can be an important mechanism by which gain may be quenched [7]. Particular emphasis has been placed on energy transfer in hydrogen halides. In a landmark study, Sirken and Pimentel [6] have examined the emission of vibrationally and rotationally excited HF ($v \leqslant 5$, $j_i \leqslant 31$, $E_{\text{internal}} \leqslant 25\,000\,\text{cm}^{-1}$) prepared inside a laser cavity from the photolytic dehydrohalogenation of vinyl fluoride and 1,2-difluoroethylene. The resulting infrared emission was dispersed in a grating monochromator and observed using a Cu–Ge photodetector, as a function of time after

the photolysis lamp flash. In the presence of $\leqslant 50$ Tor of He, Ne, or Ar buffer gas, copious lasing was observed on a number of rovibrational transitions. In explanation of the observed population inversions, the authors have proposed that low j levels of the nascent HF are transferred to nearly resonant (i.e. nearly isoenegetic) rotational levels with high j but lower v. In these vibrationally relaxed, but highly rotationally excited levels the rotational spacings are much larger than kT and the rotational relaxation processes are thus anticipated to be slow. As a consequence, the HF is effectively trapped in these excited states, creating sufficiently long-lived gain for lasing to occur. Consistent with this picture, laser gain was observed to occur more rapidly with increasing rare gas pressure, and to occur with increasing efficiency as the collider gas mass is raised.

Taatjes and Leone [67] have further quantified these assertions in studies of rotational relaxation in HF ($v = 0, j = 13$) + He, Ne, Ar, Kr, Xe, H_2, and D_2. In this work, a cell of HF/M was excited with light from a pulsed infrared laser operating at $\sim 2{\cdot}5$ μm, creating a transient population in HF($v_i = 1, j_i = 4$). The concentration of HF($v = 0, j_i = 13$), populated directly via V–R energy transfer with the buffer gas, was monitored in the time domain with direct absorption of narrow bandwidth, tunable, c.w. infrared laser light at 3 μm. The resulting time-resolved absorption traces were modelled with a simple kinetic scheme to obtain the relaxation rate constants $k_{j=13\to f}$ (that is, $j_i = 13$, several j_f), and by scaling to the mean collision velocities, the cross-sections $\sigma_{j=13\to f}$. For the rare gas sequence He, Ne, Ar the cross-sections drop as $0{\cdot}94 \pm 0{\cdot}1$, $0{\cdot}28 \pm 0{\cdot}05$, and $0{\cdot}13 \pm 0{\cdot}02$ Å^2. Note that this trend opposes the increase of $\sigma_{i\to f}$ with increasing mass that would be expected from angular momentum constraints, but can instead be explained on energetic grounds. Due to the large ($\sim 550\,\mathrm{cm}^{-1}$) spacing between the closest levels ($j = 12, 13$) with respect to kT, these relative magnitudes can be quite well reproduced with a purely impulsive model based on a Schwartz, Slawsky, and Herzfeld treatment [68], with a characteristic length-scale for the repulsive interaction that is proportional to the van der Waals radius [68]. For Kr and Xe, however, the cross-sections increase with increasing mass ($0{\cdot}70 \pm 0{\cdot}08$ and $1{\cdot}00 \pm 0{\cdot}1$ Å^2 respectively), an observation that is not readily explained. For the diatomic collision partners, cross-sections of $5{\cdot}9 \pm 1{\cdot}2$ and $8{\cdot}7 \pm 1{\cdot}7$ Å^2 were determined for H_2 and D_2 respectively, i.e., considerably higher than those for the rare gases, presumably due to the accessibility of R–R pathways.

Several studies have been carried out to measure rotational energy transfer in vibrationally excited HF. Hinchen and Hobbes [69] have used light pulses from an HF laser to pump HF($v = 1, j_i$); the ensuing collisional redistribution of population into a series of j_f states was monitored by direct, time resolved absorption of light from a second, continuous wave HF laser tuned to the peak of the desired $v = 2 \leftarrow 1$ rovibrational transition. The time dependent absorption signals were fitted to single exponential rates of growth. The state-to-state cross-sections were then modelled from the pressure-dependent risetimes, assuming that the predominant collision partner is HF($v = 0$) and that $k_{i\to f}$ follow an exponential dependence on energy gap. For levels with $j_i \leqslant 7$, the total loss cross-sections are $\sim 10^3$-fold faster than pure vibrational relaxation. Large quantum changes with $\Delta j \leqslant 7$ were observed, with transitions of $|\Delta j| = 3$ contributing as much as $\sim 20\%$. This is a striking observation, in view of the fact that if dipole–dipole forces dominate the intermolcular interaction, a selection rule $|\Delta j| = 1$ is predicted [70]. These studies were extended by Copeland and Crim [71, 72] who used a pulsed HF *overtone* laser to pump HF($v = 2$), and a c.w. HF probe laser to monitor the time-resolved transient *gain* from population in $v = 1 \leftarrow 2$ transitions.

Both exponential energy gap and power gap scaling laws were invoked to model the time- and pressure-dependent signals; either model could reproduce all data to within roughly 30%. As a consequence, large uncertainties were reported for the state-to-state rate constants, but the importance of multi-quantum changing collisions, and the rapid decrease in $k_{i\to f}$ with increasing Δj, were again clear.

In a related study, Menard-Bourcin, Delaporte, and Menard [73] have investigated rotational relaxation in $HCl(v=1,j_i=4,5,6) + HCl(v=0)$ using a similar pulsed infrared laser pump, c.w. infrared laser probe technique. Under the assumption that the state-to-state rate constants follow and energy-gap-based scaling law, the time resolved signals were fitted to extract the state-to-state rate constant matrix, extrapolated to levels not directly prepared or probed in the experiment. Here again, the importance of multiquantum changes is evident, with rate constants for $\Delta j = 2$ reported to be only ~ 2 to 3 times smaller than those for $\Delta j = 1$. Because the individual, state-to-state processes were not monitored independently, and only a subset of possible energy transfer channels were monitored with this technique, it is difficult to assess the quantitative accuracy of the elements of the rate matrix.

In order to measure the $HCl(v=1) + HCl(v=0)$ cross-sections directly, Rohlfing, Chandler, and Parker [74] have performed measurements in a regime of low collision number. In these experiments, a sample of $H^{35}Cl(v=1,j_i \leqslant 6)$ was prepared via stimulated-Raman pumping with pulsed laser light. After a short time delay, the $HCl(v=1)$ was state-selectively ionized with light from a second, pulsed laser; the ion signal was then monitored in a time-of-flight mass spectrometer. By working at sufficiently low pressures and small pump-probe time delays the probability of sequential collisions was minimized. The final state populations, observed at several cell pressures and delay times, were fitted to the analytical solutions to the state-dependent rate equations. In this manner, the state-to-state rate constants were determined without any prior constraints based on assumed scaling relations. The rate constants are quite large, on the order of gas kinetic. Interestingly, subsequent attempts to fit the rate constants to energy gap scaling formulas, such as those employed by Menard-Bourcin *et al.* [73], resulted in poor representations of the data, significantly underestimating the rate constants for larger quantum changes at high j. In fact, the values of $k_{i\to f}$ with $\Delta j = 3$ are as large as $\sim 30\%$ of those for $\Delta j = 1$, despite the rather large energy spacings between HCl rotational levels.

Chandler and Farrow [75, 76] have used a similar Raman pump/resonance enhanced multiphoton ionization (REMPI) probe technique to determine rotational energy transfer rate constants in $HD(v=1,j_i) + HD(v=0)$, and $H_2(v=1,j_f) + H_2(v=0)$. The state-to-state cross-sections for HD were used to test the accuracy of exponential energy gap models for the dependence of $k_{i\to f}$ on the rotational inelasticity. The data were most accurately represented if the energy gap model was restricted to m_j-conserving collisions, suggesting that the magnetic quantum number is not readily changed in a collision (see below). In the H_2 studies, only even Δj transitions are observed, as required if the signs of the nuclear spins are not changed in the collision. Resonant, R–R processes appear to dominate the energy transfer for $j = 0 \to 2, j = 1 \to 3$. Transfer from $o\text{-}H_2(v=1)$ to $p\text{-}H_2(v=0)$ is also observed, and attributed to V–V exchange between ground and excited H_2 of opposite spin parity; this process occurs with $\sim$ two orders of magnitude slower rates than are measured for the R–R processes.

In systems wherein the collision partners are non-polar, higher Δj transitions can take on increased importance. For example, Sitz and Farrow [77] have measured state-to-state rate constants for $N_2(v=1,j_i=0\text{–}14) + N_2(v=0)$; in this work, the

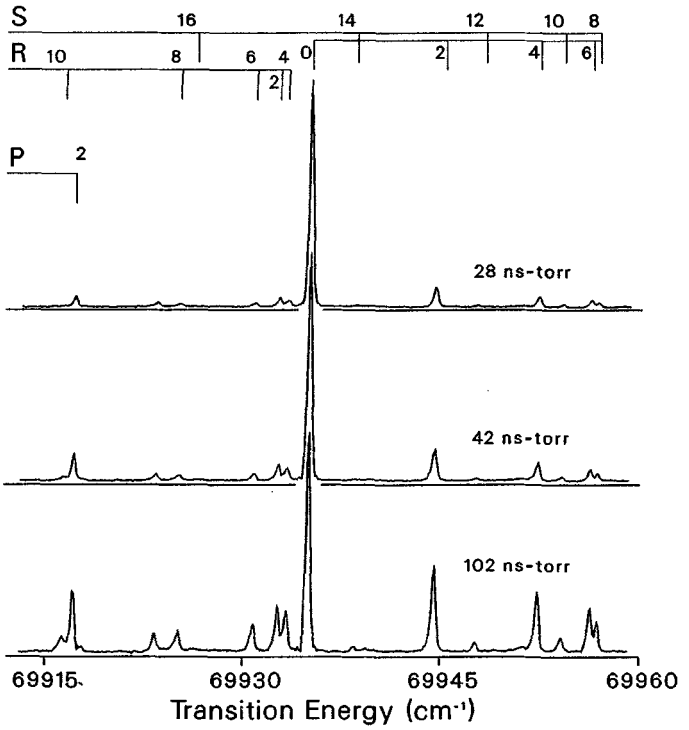

Figure 4. Time-dependent, multiphoton ionization spectra of $N_2(v = 1, j_f)$ at three pressure-time products, following excitation of the $Q(0)$ Raman transition ([77]). The growth of population with $j_f \neq j_i$ due to rotationally inelastic collisions is evident by the appearance of satellite bands. The spectral intensities reflect the state-to-state rate constants for rotational energy transfer.

excited N_2 was prepared using stimulated-Raman pumping, and probed via $2 + 2$ resonance-enhanced, multiphoton ionization (figure 4). Energy transfer with Δj as large as $\pm$ 12 was observed, restricted by symmetry to even values. The rate constants exhibit a steady decrease with increasing energy gap, but this decline is considerably slower than is observed in HF or HCl (above). Because N_2 has no permanent dipole moment, the relatively high probabilities for large rotational inelasticities may reflect high-order, electrostatic contributions to the intermolecular potential, in contrast to the propensity for $\Delta j = 0, \pm 1$ transitions expected when dipole–dipole interactions dominate. Efficient transfer for large Δj is also likely to be facilitated by the small rotational constant for N_2 ($\sim 2\,cm^{-1}$), as large changes in rotational state imply relatively small energetic differences. The experimentally determined $k_{i \to f}$ were fitted to several energy gap scaling formulae; a statistical polynomial model [78] and an energy corrected sudden model [79] were both found to reproduce the data with reasonably high accuracy.

In summary, rotational energy transfer in ground-state molecules can be quite state-specific, often with large transition probabilities for multi-quantum jumps that often are not readily predicted from simple assumptions energy gap formulations, or dominated by dipole–dipole selection rules. For strong collisions driven predominantly by dipole–dipole forces, energy transfer in a symmetric top such as ammonia can exhibit propensities for Δj, Δk, and for preservation of parity with respect to inversion.

For weaker collisions in which higher electrostatic moments dominate, such fine structure selectivity can be largely washed out. However, the symmetry of the interaction potential can impose simple selection rules, e.g. $\Delta k = 0, 3, 6 \ldots$ for NH_3 + rare gases.

4.3. *Energy transfer within vibrationally excited polyatomic molecules*

When a polyatomic, symmetric (or spherical) top molecule is excited into a doubly degenerate (or n-fold degenerate) vibrational level, rotation of the molecule induces a Coriolis force that results in vibrational angular momentum l. This vibrational angular momentum, which classically corresponds to a clockwise or counterclockwise orbit of each nucleus about its bond axis, can provide an additional source/sink for collisional transfer of rotations. To investigate the mechanisms that underlie the collisional interchange of molecular tumbling motions with vibrational angular momentum, and also to provide the first state-resolved energy transfer rates for spherical top molecules, Steinfeld and coworkers have carried out studies of rotational energy transfer in $^{13}CD_4$ and silane [20–23]. Light from a pulsed CO_2 or Raman-shifted Ti ; sapphire laser was used to prepare the target molecule in a particular rotational level of a degenerate vibrational state. The temporal evolution of a number of rovibrational levels was monitored using direct absorption of narrow-bandwidth, near-infrared light from a tunable diode laser.

Quite large changes in rotational quanta, with $\Delta_j \leqslant 5$, were observed. As might be expected for collisions between paramagnetic molecules, the fine structure levels delineated by their A, E, or F nuclear spin symmetries do not interconvert. Of more dynamical significance, although a large number of quantum levels are energetically accessible a remarkably limited subset are populated to any appreciable extent. The authors identified a number of 'principal' pathways through which energy transfers occurs preferentially (figure 5). Since many of these states are nearly isoenergetic with levels that are *not* among the principal pathways, this selectivity cannot be explained from energy gap arguments. The principal final states are, however, inevitably limited to those levels such that the vibrational angular momentum vector is unaltered in the collision. Physically, this implies a conservation of the vibrational angular momentum in the molecular frame. In other words, the handedness of the orbits executed by the D atoms is not readily reversed in a collision.

Taken alone this explanation overpredicts the number of principal channels. To account for the remaining specificity, Parson [80] has demonstrated the importance of an additional, constraining mechanism as follows. In the excited, triply degenerate v_4 state the methane (or silane) undergoes centrifugal distortion about one of its symmetry axes. On sufficiently short time-scales, e.g. the duration of a collision, the distorted molecule acts as a *symmetric* top, with a quantum number k_r labelling the projection of the angular momentum about the symmetry axis. Although not necessarily obvious, the relevant quantization direction is not along one of the bond axes with C_3 symmetry, but rather along a fourfold axes for improper rotation in the T_d rotation group. Therefore a selection rule of Oka (see above) for symmetric top molecules, in which changes in k are limited to the integral multiples of the order of the symmetry axis, can be applied to k_r. Specifically, for methane and silane, $\Delta k_r = 0 + 4n$ or $2 + 4n$ depending on nuclear spin symmetry. Almost all the fine structure selectivity is taken into account under this interpretation. If this picture is accurate, and the existence of principal pathways reflects the internal structure of the methane rather than the details of the interaction potential, one anticipates different, but

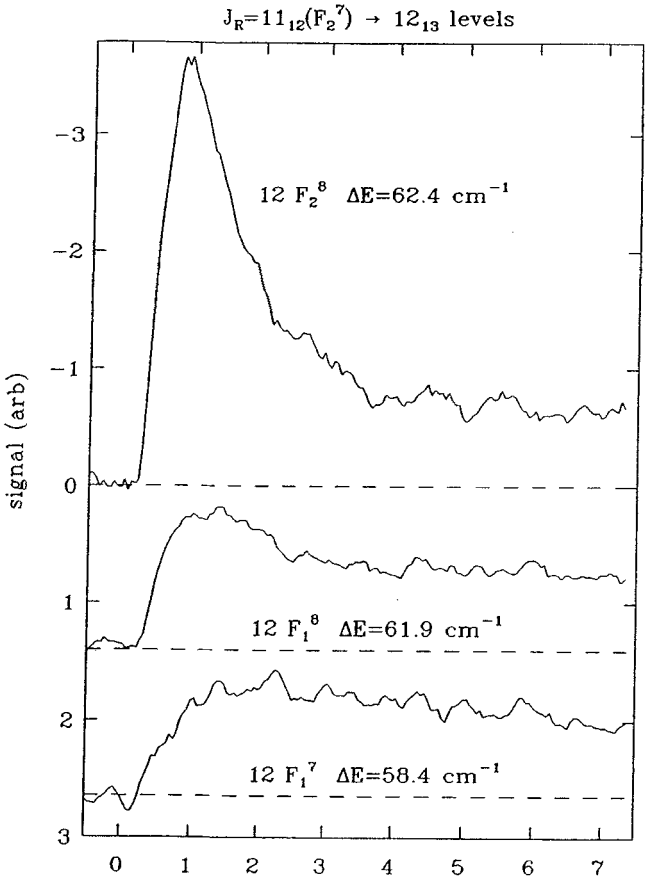

Figure 5. Typical time resolved, infrared laser absorption traces for several rotational levels in vibrationally ($v_4 = 1$) excited CD_4 ([20]). In the labels for each trace, the number 12 indicates that a $j_f = 12$ state is probed; the remaining quantum state label identifies the symmetry species. The absorption traces show the time-dependent population transferred to each state in collisions with ground state CD_4, following the preparation of $j_i = 11$ (F_2^7). Note that although all three final states shown have equal j, the observed populations, and hence the state-to-state cross-sections, vary dramatically among them. The top trace (largest amplitude signal) represents a principal channel, and differs from the middle and bottom in its vibrational angular momentum. Such state-specificity can be understood almost entirely from the symmetry of the CD_4 (see text).

equally state-selective, energy transfer for a methane isotope with lower symmetry. Indeed, in studies of energy transfer in the intrinsically symmetric top CHD_3, Klaassen *et al.* [23] have observed the expected propensities for $\Delta k = 0, 3$, with the final state selectivity predicted from the symmetry of the molecule. Intriguingly, then, energy transfer in a spherical top such as methane or silane reflects the internal structure of the target molecule, and is quite independent from details of the short-range forces that might be expected to govern rotational energy transfer.

Relatively little is known about energy transfer in asymmetric top molecules. Orr and coworkers [81–85] have investigated energy transfer in vibrationally excited D_2CO and HDCO, by optically pumping $j_i = 18$, $k_a = 11$, k_c, in the $v_4 = 1$ vibration; the product state populations were measured via LIF. Because ortho and para spin

modifications are not interconverted in a collision, only transitions with even values of Δk occur. Quite large changes in j were observed, with as many as seven quanta exchanged in a single collision. The state-to-state rate constants are reasonably well described by energy gap fitting expressions, provided that large Δj are allowed, further supporting the importance of multi-quantum changes. Self-relaxation of the formaldehyde proceeds at a significantly faster rate than does quenching by the foreign gases He, Ar, N_2 and N_2O, presumably due to resonances in the R–T, R energy transfer process.

A burgeoning field of research has been rotational energy transfer in molecules at high levels of vibrational excitation where the density of states ρ, and hence the number of energetically available energy transfer channels, can be quite high. If ρ is unduly large, however, the vibrational excitation spectrum will be too dense to allow rotationaly resolved energy transfer studies to be carried out. Excitation of CH stretch overtones (ν_{CH}) in actylene, at $\leqslant 10\,000\ cm^{-1}$, provides a density of states that is sufficiently large ($\rho \leqslant 3$ states/cm^{-1}) to investigate competing vibration-to-vibration, rotation (V–V, R) processes, but sufficiently sparse to allow individual rovibrational states to be probed. Lutz *et al.* and Tobiason *et al.* [86, 87] have used direct, pulsed laser overtone excitation to prepare $C_2H_2(m\nu_{CH}, m < 4, j_i \leqslant 22)$ in a gas cell. The population in a given j_f was monitored via LIF, at a series of time delays after the vibrational excitation, following collisional energy transfer with ground state C_2H_2, He, Ar, or Xe. Total loss rate constants from the optically prepared state (i.e., $j_i \rightarrow \Sigma j_f$) were determined from Stern–Volmer plots of the observed decay rates as a function of cell pressure. State-resolved rate constants $k_{i\rightarrow f}$ were determined, under predominantly single collision conditions, from the LIF signals, at a series of pressures and time delays.

The self-relaxation rate constant k_{self} for C_2H_2 is large, on the order of gas kinetic. This rate constant varies by $\leqslant 20\%$ over the range $8 \leqslant j_i \leqslant 20$. Despite an order of magnitude change in the density of states, k_{self} is essentially independent of the vibrational level. This result indicates that at these state densities, intramolecular relaxation processes play a subsidiary role in the decay of the nascent excited state population. Furthermore, the rate constants for relaxation by the rare gases are almost half as large as k_{self}, despite the rate enhancement one might expect due to efficient V–V transfer in $C_2H_2 + C_2H_2$ collisions. Therefore, it appears that vibrationally inelastic energy transfer is also of secondary importance in the disposal of excess energy. Consequently, rotational energy transfer must be the dominant relaxation process. This hypothesis was subsequently verified [87], by measurements of state-to-state rate constants within a single vibrational manifold: the sum of all significant $k_{i\rightarrow f}$ accounts for $\sim 70\%$ of the total loss rate constants.

In the state-resolved measurements, the values of $k_{i\rightarrow f}$ decrease monotonically with increasing Δj. Because the nuclear spins of the H atoms are not flipped in the collisional encounters, only even changes in j are observed. Although the largest rate constants are those with $\Delta j = \pm 2$, transitions with Δj as large as ± 20 are observed. This result is in interesting contrast with the studies of Temps *et al.* [88, 89] of rotational relaxation in vibrationally excited formaldehyde, where $\Delta j = \pm 1$ transitions account for $\sim 90\%$ of the inelastic collisions. This difference may stem from the permanent dipole moment of formaldehyde, as a $\Delta j = \pm 1$ propensity is predicted when dipole–dipole forces dominate the interaction potential. For the non-polar acetylene, energy transfer presumably occurs largely through short-range, repulsive interactions where higher multipole moments are significant.

In brief summary, state-resolved, rotational energy transfer in polyatomic molecules

is a relatively unstudied arena. Rotational energy transfer in polyatomics can be quite efficient, dominating inter- and intra-molecular vibrational relaxation rates. The existence of resonant, or near resonant, energy exchange channels can enhance the already-large rates at which rotationally excited molecules relax. Furthermore, the predominant energy transfer channels can be quite specific in their final j and fine structure states, reflecting internal symmetry of the target molecule.

4.4. m_j-*changing collisions*

Relatively little experimentation has addressed the rates and propensities for m_j-changing collisions in electronic ground states. Quite recently, Sitz and Farrow [90] have reported measurements of the collisional relaxation in an aligned sample of molecular nitrogen. $N_2(v = 1, j_i = 0, 2, 4, \ldots, 14)$ was prepared with an anisotropic m_j distribution via pulsed, stimulated-Raman pumping on S branch transitions. After a suitable time delay, the population of $N_2(v = 1, j_f)$ was probed by REMPI with another laser; the resulting ion current was detected in a parallel plate electrode assembly. From the dependence of the REMPI signal intensity on the angle between the pump and probe laser polarization vectors, the m_j distributions that accompany rotationally inelastic collisions were extracted. The initial m_j distributions persist, largely undisturbed, on the time scale of many j-changing collisions. Calculations of the expected alignment for $j_i = 6 \rightarrow j_f = 4$, assuming $\Delta m_j = 0$ as suggested by the group of McCaffery for electronically excited I_2 and Li_2 (see above), underestimate the observed quadrupole moment of the observed m_j distribution in $j = 4$. The intuitively appealing idea that the classical angle θ remains unchanged (equation 5) gives better agreement with the experimental results, although this approach leads to an unphysically structured distribution of m_j levels. If the restriction on θ is loosened such that arbitrary changes in this angle are allowed, but with probabilities that decrease in inverse proportion to $\Delta\theta$, a smoother m_j distribution is predicted that gives better agreement with experiment. In any event, these experiments lend strong support to the idea that m_j states are not readily changed in a collision due to a tendency to preserve the orientation of the j vector.

4.5. *Energy transfer between spin–orbit states*

NO has been a particularly attractive free radical for studies of rotational energy transfer. In contrast with most radical species it can be stored in a thermal cell, undepleted by reactive loss, for long periods of time. Furthermore, NO is sufficiently small to be amenable to *ab initio* calculations, thus opening up the possibility of direct comparisons of experiment and theory. Sudbø and Loy [91] have measured state-to-state cross-sections for $NO(X^2\Pi, v = 2, j_i)$ + NO, He, N_2, CO, and SF_6 with a double resonance scheme that takes advantage of the low ionization potential of NO [92]. In a static cell with the collision partner of choice, NO was pumped into various j_i in $v = 2$ with a tunable, pulsed colour centre laser. After a suitable time delay, NO $(v = 2, j_f)$ was ionized with an intense ultraviolet laser pulse; the ion current was detected in a parallel-plate electrode assembly, providing a measure of the final state population. The state-to-state cross-sections fall off quite slowly with increasing Δj, independent of the initial state excited. In particular, although a selection rule of $\Delta j = 0, \pm 1$ would adhere if the energy transfer were dominated by the permanent dipole moment of the NO, no such propensity holds true. For self-relaxation of NO, spin–orbit changing and preserving collisions were found to occur with equal probabilities. For the remaining gases a propensity was observed for collisions to preserve the spin–orbit

state, an effect observed most strongly in He. One possible conclusion is that spin–orbit changing collisions are more facile events when a collision complex is likely to be formed due to a strong attractive forces, and thus are more likely with the dipolar NO than with the very weakly polarizable He.

Yang and Wodtke [93] have extended self-relaxation studies of NO to highly vibrationally excited levels. The excited NO($v_i = 8, 19, j_i$) was prepared using stimulated emission pumping (SEP); the population of NO(v_i, j_f) was monitored, as a function of (predominantly ground state) NO pressure, using laser induced fluorescence (LIF). For both spin–orbit manifolds, the state-to-state cross-sections decrease with increasing Δj; the relaxation is dominated by collisions with $\Delta j = \pm 1, \pm 2$. Interestingly, the observed values of $\sigma_{i \to f}$ are, to within $\sim 20\%$, independent of the vibrational state ($v_i = 8$ or 19) initially prepared. Therefore, rotational energy transfer within a given vibrational manifold is essentially unaffected by the vibrational motion, even at internal energies as large as $\sim 31\,000\,\text{cm}^{-1}$.

4.6. *Collisions with translationally energetic atoms*

Most of the methods discussed so far provide means to study rotational energy transfer at thermal energies, that is, for mean collision energies on the order of a few hundred wave-numbers. Although some variability can be provided by heating or cooling the thermal cells, this tuning range is limited and it is therefore difficult to access chemically significant energies on the order of electron volts with these techniques. In order to generate collisions in this higher range of E_{coll}, several groups have utilized schemes using laser flash photolysis, in a long flow cell, of a precursor chosen such that one photofragment is a translationally energetic atom (or, in principle, molecule). The translational energy is subsequently transferred to internal modes of an infrared absorbing target gas M. The final state distributions of M are probed as a function of time and quantum state via weak fractional absorption of narrow band, c.w. radiation from a continuously tunable, infrared laser that illuminates a known path length collinear with the photolysis laser. The intensities of the transient infrared absorption (or in principle, gain) signals are related to the population difference between v'', j'' and v', j' via Beer's law, if the upper vibrational state is unpopulated, the signal intensities provide a direct measure of the population of $M(v'', j'')$.

Flynn and coworkers have used such an approach to investigate rotationally and vibrationally inelastic collisions of $CO_2 + H$, D in which the hydrogen atoms were produced in a relatively narrow translational distribution with 193 nm excimer laser photolysis of H_2S/D_2S (mean $E_{\text{coll}} \sim 2\,\text{eV}$) [94–103]:

$$H_2S + h\nu(193\,\text{nm}) \rightarrow H^* + HS, \tag{7}$$

$$H^* + CO_2(00^00, j_i) \rightarrow CO_2(1m^0p, j_f) + H, \tag{8}$$

with analogous equations for the D isotope. The populations of $CO_2(1m^0p, j_f)$ were monitored using a lead salt diode laser at 4·3 μm:

$$CO_2(1m^0p, j_f) + h\nu(4{\cdot}3\,\mu\text{m}) \rightarrow CO_2(1m^1p + 1, j_f + 1).$$

From the transient infrared signals taken at early times ($\sim$ 1–2 μs, close to the $\sim$ 700 ns response time of the infrared detector) corresponding $\sim$ one gas kinetic collision, efficient T–R transfer was observed. For H atoms at 2·3 eV the rotational distribution in $CO_2(00^01)$ peaks at $j_f \sim 32$, as compared with ~ 18 for the nascent thermal distribution; states as high as $j_f = 48$ were observed. With D atoms at 2·2 eV even greater

rotational excitation was observed, with $j_f \leqslant 64$, presumably due to the higher reduced mass compared to H + CO_2, and hence the greater orbital angular momentum for a given impact parameter. For $CO_2(00^00, j_f \geqslant 54)$, the populations for a given j_f are larger for D* than for H* by a factor of roughly two, with a small but significant dependence on rotational state. Interestingly the state $(00^00, j_f = 78)$ is populated with higher probability by D, whereas energy transfer into the nearly isoenergetic level $(00^01, j_f = 13)$ occurs more readily for H. These observations again indicate that D atoms are more efficient at populating higher j states, and that the dynamics are not driven solely by energy gaps.

When the $CO_2(01^10)$ doubly degenerate bending state is probed following collisions with D atoms [96], the populations in highly excited, *odd j* levels are roughly twofold higher than the populations in neighbouring *even* states. At colder temperatures (~ 223 K) where the nascent populations in this bend state are significantly reduced, the odd j levels are even more heavily favoured. Since the CO_2 in its linear ground state has only even j states, it appears that collisional excitation into the v_2 bending level is accompanied by rotationally inelastic events with a strong propensity for odd Δj.

From the above arguments, collisions with a heavy atom such as Cl might be anticipated to produce highly rotationally excited final state distributions. Quite different results have been obtained, however, by Zhao *et al.* [104] in studies of Cl* + HCl($v = 0, j$). In this work the energetic Cl was created from Cl_2 photolysis using 308 nm light from a XeCl excimer laser. The rotational population distributions of HCl bath gas were monitored via time- and frequency-resolved absorption of narrow bandwidth, continuously tunable light from an infrared colour centre laser. For low rotational states that are populated in the nascent, thermal distribution of HCl(j_i), the Doppler profiles observed at short times after the photolysis flash exhibit distinct depletion near line centre but increased amplitude at large Doppler detunings (figure 6). These observations reflect a constant, fractional *loss* probability across a narrow 300 K Doppler width, offset by a substantially broader Doppler profile for *growth* into a given state; for high j states, of course, only growth is observed. The relative changes in population were determined by fitting the line-shapes to the sum of two contributions: a negative going Gaussian constrained to a 300 K Doppler profile to represent collisional loss, and an arbitrarily broad Gaussian to account for growth. The integrated area under the loss profile then gives the integral cross-section out of a given j_i, summed over all j_f; similarly, the area under the growth curve gives the cross-section into a given j_f summed over all j_i.

At the mean collision energy of $\sim 3500\,\mathrm{cm}^1$ the loss and growth cross-sections decrease with increasing j_i or j_f. Essentially all the population is observed in states with $j_f \leqslant 12$, a substantially lower value than the energetic limit of $j_f \sim 18$. Moreover, the root mean squared energy transferred per collision is less than 10% of the $3500\,\mathrm{cm}^{-1}$ mean energy, a value that is clearly not limited by the $\sim 76\hbar$ of orbital angular momentum available for a reasonable impact parameter of 1·27 Å. In explanation the authors suggest that at high j_f, the rapid rotation of the HCl with respect to the collision period effectively washes out the angular anisotropy of the potential, inhibiting the population of states with $j_f > 12$. Quasi-classical trajectory calculations, performed on a potential of Schatz and Gordon, further indicate that most collisions are direct and involve little transfer of rotation. A small subset of trajectories lead to formation of a potentially reactive collision complex, however, which in turn lead to highly rotationally inelastic scattering or can dissociate into Cl atom exchange products. The observations that few reactive exchanges occur, and that high j states are largely

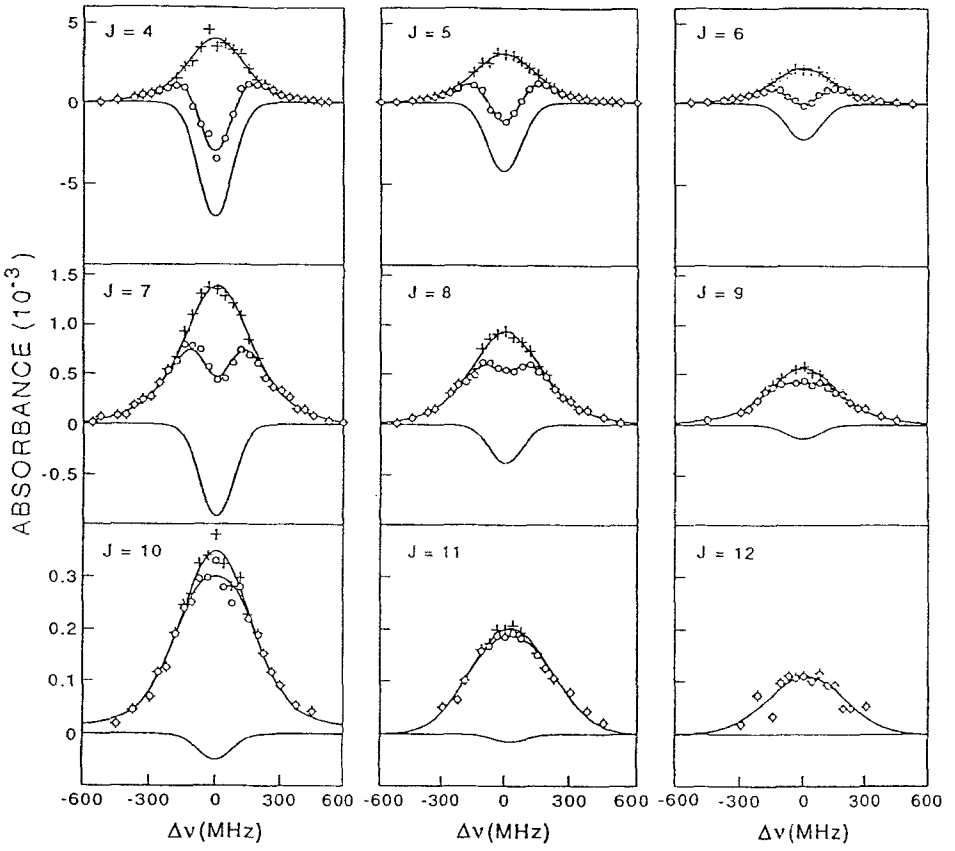

Figure 6. Line-shapes observed by infrared laser Dopplerimetry in the inelastic scattering of Cl + HCl ([104]). For thermally populated, low j states, the Doppler profiles result from the competing effects of collisional loss to other states, and growth from other states. The rates of total loss out of, or growth into, a given rotational state, j, are determined by decomposition of the observed line shapes into these components.

unpopulated, buttress the interpretation that large rotational excitations are produced via dissociation of a relatively long lived complex.

In summary, the energetic transfer of atomic momentum to rotation of a molecular target gas can proceed more efficiently with increasing mass, due to increased reserves of orbital angular momentum. At sufficiently high mass, however, rotational averaging effectively reduces the anisotropy of the potential, precluding the formation of high j states. The concomitant excitation of a vibration and a rotation can result in additional, state-specific dynamics, as exemplified by the even–odd intensity alternations for $D + CO_2$.

5. Crossed beam studies

5.1. *Background*

In the types of experiments described thus far, wherein a non-thermal sample of molecules is allowed to come to equilibrium through collisions with a thermal bath gas, the cross-sections for collisional energy transfer are inherently integrated over broad spreads of collision energies, centre of mass velocities, and internal states of the collider

gas. Since this level of thermal averaging can mimic that of flames, planetary atmospheres, or chemical lasers, the resulting cross-sections can often be applied quite directly to models of such chemical systems. Often, however, it is desirable to define the collisions conditions more precisely. For example features such as glory oscillations and scattering resonances, which can be observed from the dependence of the integral cross-section on collision energy [26, 105], are generally obscured by the wide, thermal distributions of molecular velocities. Moreover, in order to measure *differential* cross-sections with which to test theoretical potential energy surfaces, one requires a well-defined axis for the collision velocity in the laboratory frame, a condition difficult to attain in a thermal cell.

In order to generate well-defined collision energies having small spreads, and to minimize the number of internal states that are populated, crossed molecular beam techniques have been instrumental [27]. By virtue of supersonic cooling in the free jet expansions, the target and collider gases are prepared in their lowest rotational states. The use of two skimmed, translationally cold beams can lead to quite small dispersion in the centre of mass collision energies, and provides a definite laboratory orientation for the centre of mass collision velocity. Furthermore, since the number densities are intrinsically low and the spatial overlap of the molecular beams small, inelastic scattering under predominantly single-collision conditions is readily achieved. In addition, by changing the angle at which the beams intersect, the collision velocity, and hence collision energy, can be tuned over a wide range.

A principle experimental challenge has been the state-selective detection of rotationally excited target molecules in the scattered flux. This has proven difficult because of the low number densities in the crossed molecular beam environment. For measurements of *integral* cross-sections, the populations in ground and excited states can be interrogated directly in the beam intersection region, with methods that have included infrared emission, pulsed laser induced fluorescence (LIF), multiphoton ionization (MPI), and infrared absorption. In the single collision limit, the state-to-state, integral cross-sections are proportional to the fraction of molecules scattered into each j_f. Since it is the scattered *flux* into each state that determines the relative cross-sections, whereas the laser based methods typically produce signals proportional to the *number density*, a j-dependent correction must usually be made [27]. The conversion of number density to flux presupposes knowledge of the differential cross-section $d\sigma/d\Omega$, as determined from experiment, *ab initio* calculations, or simple classical models. The relative values $\sigma_{i\to f}$ are extracted from the j-dependent fluxes as a function of collider gas concentration.

In order to determine *differential* cross-sections, one requires a measurement of the angle-dependent flux. In one method that dates back well over a decade [106–110], the target and collider gases are supersonically cooled in chopped molecular beams, producing gas pulses several microseconds in duration. The scattered target gas is detected as a function of laboratory angle in a rotatable, time-of-flight, mass spectrometer. By conservation of energy in the T–R collision process, target molecules with increasing rotational excitation move more slowly, and appear in the mass spectrum at increasing time delays. The time-of-flight spectrum can therefore be mapped into an energy loss spectrum, from which the j-dependent, differential cross-sections may be inferred. A significant advantage of the time-of-flight methods is generality, in that they can be used to detect virtually any target gas.

Several complicating factors in the analysis are worth mentioning. In principal, for an atomic collider gas the arrival time for each successive j state can be determined

uniquely, and the j_f label of each peak in the time-of-flight spectrum unambiguously assigned. For a molecular collider, however, additional collision energy may be taken up in internal modes and the time-of-flight mass spectrum may not be single-valued, potentially complicating the analysis of state-to-state cross-sections. Moreover, the effective energy resolution is typically limited to ~ 10–$100\,\mathrm{cm}^{-1}$, depending on the masses of the colliding species. For molecules with sufficiently large rotational constants and light collider gases, this can prove sufficient to allow the state-to-state cross-sections to be determined. More commonly, however, the peaks in the time-of-flight spectrum are heavily overlapped, precluding extraction of the *state-to-state*, differential cross-section. From the time-integrated intensity as a function of angle, however, the *total* (i.e., summed over all j_f), differential cross-section can be determined. The angular resolution can be as high as $\sim 1°$ under favourable conditions, sufficient to resolve rainbow structure and diffraction oscillations in the differential cross-sections.

To measure differential cross-sections at the state-to-state level of detail, several authors have developed laser based methods. Since molecules that are scattered into a given, centre-of-mass angle have a characteristic velocity component along the laser axis, the differential cross-section is manifested in the shape of the Doppler profiles. Kinsey [111] has presented a method for the determination of $d\sigma/d\Omega$ through Fourier transform of the Doppler profiles; a more mathematically refined method of analysis, for cases with cylindrical symmetry, has been presented by Taatjes *et al.* [112]. For a laser probe directed parallel or perpendicular to the relative, centre-of-mass velocity vector, Serri *et al.* [113, 114] have developed a straightforward formalism for extraction of $d\sigma/d\Omega$ from the observed Doppler line shapes without any intermediate journeys into Fourier space. In a more direct approach, Bergmann [115] and ter Meulen [116] have introduced rotatable, fibre optic based, LIF detectors in which the scattered target molecules are probed on their Newton spheres well outside of the beam intersection region, thus probing the angle-dependent scattering directly (figure 7 (*a*)). In short, a variety of laser-based methods exist for the determination of state-resolved, differential scattering cross-sections for rotationally inelastic energy transfer.

5.2. *Integral cross-section measurements: diatomic molecules*

Several early studies of rotational energy transfer in $HCl(v = 1, j_i)$ and in $HF(v = 1, 2, j_i)$ were performed by Polanyi and coworkers [117–120], with an 'arrested relaxation' technique in which the target gas, seeded in a supersonic beam and rovibrationally excited by heating the nozzle or by optical excitation with an HF laser, interacts with a spatially divergent, pulsed jet of collider gas. The j_f-dependent populations in the vibrationally excited state, which were partially relaxed from the collisional interaction, were monitored via dispersed, infrared emission spectroscopy. The state-to-state cross-sections are found to decline rapidly with increasing j and Δj, providing some of the earliest evidence that the efficiency of rotational energy transfer can drop off markedly with increasing energy gap. A similar interpretation was given by Sung and Setser [121] for the highly non-thermal populations of $HF(v \leqslant 3, j_f)$ or $HCl(v \leqslant 3, j_f)$, prepared as the products of fast chemical reactions and collisionally redistributed by Ar collider gas. The resulting rotational states are largely bimodal, with two broad peaks centered at low $j \sim 3$ and high $j \sim 15$–25. The longevity of population in $j_f \geqslant 10$, where the energy level spacings are larger than kT, is interpreted at a bottleneck in the rotational relaxation process due to the rapidly declining energy transfer rates at high j.

Despite the large rotational constant of HF ($b_{HF} \sim 20\,cm^{-1}$) and hence the large energy spacings between adjacent rotational levels, modelling of the observed j_f populations in these experiments indicates that multiquantum jumps (i.e., $\Delta j > 1$) contribute significantly to the relaxation process. The rotational state distributions of HF are quite similar for the rare gas colliders Ne, Ar, and Kr, indicating that the relative, state-to-state cross-sections do not differ markedly among these atoms despite their widely differing masses and polarizabilities. In collisions with HCl, however, HF is substantially more relaxed presumably due to the importance of efficient, rotation–rotation energy transfer channels and the strong, dipole–dipole interaction.

Andresen *et al.* [122] have used a crossed beam apparatus in conjunction with pulsed, LIF detection to monitor rotational excitation of $NO(X^2\Pi, n = 0, j = 0{\cdot}5) + Ar$. As a general trend, the integral cross-sections decrease slowly with increasing n_f.

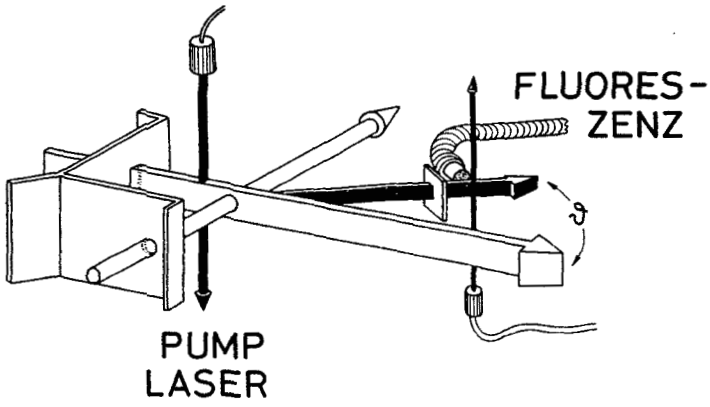

(*a*)

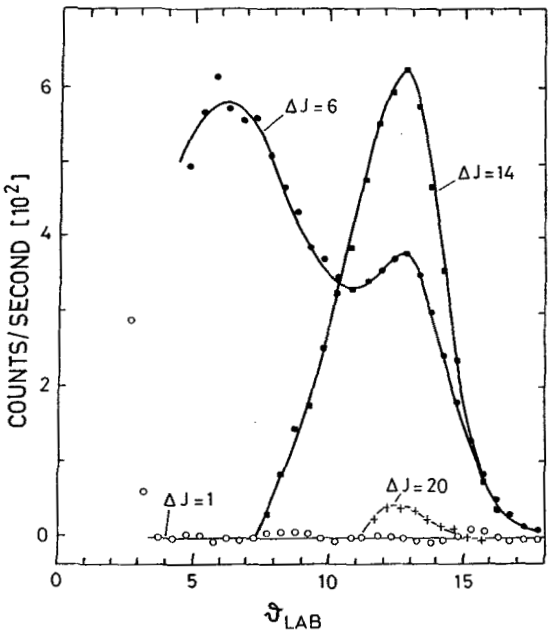

(*b*)

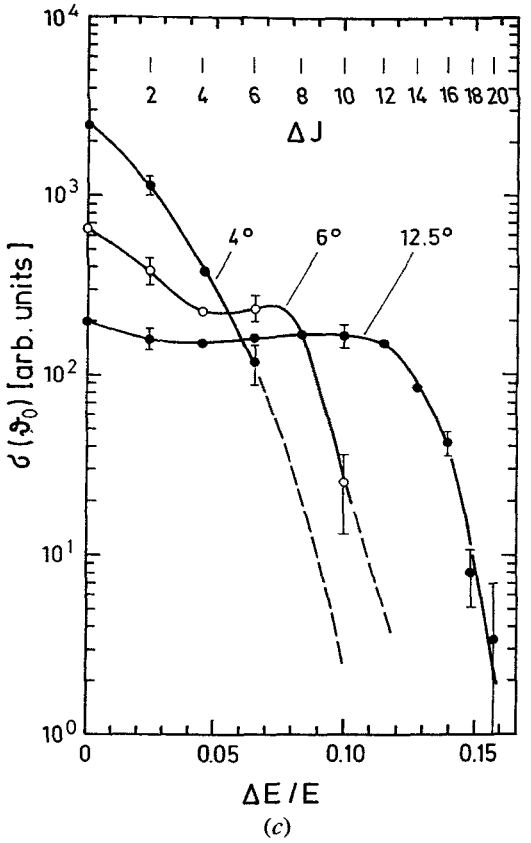

Figure 7. Laser-based differential cross-section measurements (from [115]). (*a*) Crossed-beam apparatus, with rotatable LIF detector. (*b*) Angular scattering in laboratory frame for $Na_2(J_f = 28)$ + He. (*c*) Dependence of the scattering cross-section on the fractional energy transferred in Na_2 + He, for several laboratory angles. The steep shoulders for $\theta_{lab} = 6°$, 12·5° are signatures of rotational rainbow scattering.

At a more detailed level, however, the values of $\sigma_{i\to f}$ exhibit intensity alternations in which even n levels are more populous than neighbouring states with odd n, for $n \leqslant 8$. At higher rotational levels, this ordering appears to reverse with slightly elevated populations in odd levels. This distinctive structure arises from the near symmetry of the Ar–NO potential with respect to interchange of the N and O nuclei, which is dominated by even terms in a Legendre polynomial expansion. This interpretation is corroborated by scattering calculations on a theoretical potential of Nielson *et al.* [123], with S matrix elements calculated with the approximate coupled-states method and treating the NO as a Σ molecule, which reproduce the qualitative ordering of the j-dependent intensities. In a complementary picture, the intensity alternations arise from interferences of the partial waves scattering from both ends of the NO. This structure, therefore, cannot be predicted using classical trajectories, but is a purely quantum-mechanical effect. Here is a clear example, then, of a case in which the dependence of $\sigma_{i\to f}$ on n_f may be determined largely by the symmetry, or near symmetry, of the intermolecular potential energy surface.

5.3. *Energy transfer in closed shell, polyatomic molecules*

The study of energy transfer in polyatomic molecules affords the opportunity to explore energy transfer among several rotational degrees of freedom. Nesbitt and coworkers [124–126] have recently studied collisional energy transfer in CH_4 + He, Ne, and Ar, in a crossed jet apparatus in which the scattered CH_4 was probed, in the intersection region, via direct absorption of narrow bandwidth, infrared laser light. In these experiments the A, F, and E nuclear spin modifications of the CH_4 are not interconverted in a collision, so that in effect three independent scattering experiments are performed. By symmetry CH_4 is a spherical top, but the tetrahedral structure ensures a somewhat non-spherical interaction potential with respect to *M*. The angular anisotropy of the potential allows torque to be generated, opening up the possibility that these surfaces might be probed by studying rotational energy transfer. The absolute cross-sections for all three rare gases are quite large (tens of $Å^2$), indicating substantial angular anisotropy in the CH_4 + rare gas potentials. The j_i and j_f dependencies of the integral, state-to-state cross-sections do not scale in any predictable way with energy or angular momentum gap. As shown from close coupling calculations, the data are fairly well predicted by existing potential energy surfaces [127–129] that account for the lowest order angular anisotropy, as derived from *ab initio* calculations and the differential scattering calculations of Buck and coworkers (see below). However, at the state-to-state level some discrepancies persist between observed and calculated cross-sections, suggesting that higher-order terms in the potentials are important. Nonetheless, from these surfaces it is seen that long range, the rare gases are drawn in more strongly towards the H atoms than to the edges or faces of the CH_4, whereas at short range the H atoms are the most strongly repulsive.

Meyer [130] has determined integral cross-sections for NH_3 + Ar, in a unique two-beam experiment. In this arrangement, the pulsed, target and collider beams are arranged in a counter-propagating geometry. The scattered NH_3 was ionized, as a function of quantum state, via pulsed laser, resonance enhanced, multiphoton ionization and detected in a time-of-flight mass spectrometer. The time-integrated signal intensity provides a measure of the state-to-state, integral cross-section. At 0·158 eV, only states with $\leqslant 40\%$ of the maximum possible energy are observed to be populated, with cross-sections that decrease with increasing Δj. For o-NH_3 the parity levels are not resolved, but for p-NH_3 both the + and − parity levels are observed, with more population in the + levels. A strong propensity for $\Delta k = 3$ is seen for − parity states. The observed, state-to-state cross-sections are well predicted by scattering calculations on an existing potential.

ter Meulen and coworkers [131–134] have carried out crossed beam measurements of integral cross-sections for NH_3 + He, Ar, and H_2. In these experiments a single j, k, and inversion level of the NH_3 is selected, with high discrimination against other states present in the nascent supersonic expansion, prior to interaction with the collider beam using a hexapole field. The scattered NH_3 was state-selectively ionized, and detected in a particle multiplier. As a general pattern the cross-sections decrease with increasing Δj. At a more detailed level, marked j- and k-dependent propensities are observed for energy transfer among states that differ in total symmetry (i.e., inversion doubling + rotational) with $\Delta j = 1$ rates enhanced for o-NH_3, and $\Delta k = \pm 3$ for o- and p-NH_3. Comparison of observed and theoretical cross-sections gives good agreement for the symmetry-averaged cross-sections, although theory predicts more dramatic symmetry preferences than are observed experimentally. Of possible relevance to the formation of interstellar NH_3 masers [135–137], the state-to-state

cross-sections for He and H_2, despite their equal masses, exhibit quite different propensities for populating the upper or lower parity doublets for a given j and k. This observation suggests that the internal degrees of freedom of the H_2 may be relevant in determining the final state of the NH_3.

5.4. *Energy transfer between spin–orbit states and* λ-doublets

The study of energy transfer in free radicals has reached impressive levels of detail, largely as a result of experiments performed in molecular beams; a review has recently been published [138]. In the realm of astrophysics, one longstanding problem has been determination of the mechanism that creates population inversion between λ-doublet states in the OH interstellar maser [139, 140]. While both optical and collisional pumping mechanisms have been proposed [8, 141–144], one dominant hypothesis has been selective λ-doublet preparation via collisions with H_2. Andresen *et al.* [140, 145, 146] have studied energy transfer of ground state $OH(X^2\Pi_{3/2}, n = 0)$, created by excimer laser flash photolysis of HNO_3 in a target molecular beam, and collisionally excited by a cold, collider beam of H_2 or D_2. The final state populations were measured via LIF, as a function of n, spin–orbit state, and λ-doublet level. The state-to-state, integral cross-sections show a monotonic decrease as j_f increases. Substantial population is transferred into the $^2\Pi_{1/2}$ spin–orbit manifold, which implies large differences between the A' and A'' Renner–Teller surfaces that govern the collision interaction, as has been shown theoretically [123, 142, 147–149]. Since these two surfaces differ in the orientation of the unpaired electron orbital, then alternatively stated, the interaction of the unpaired electron with the H_2 molecule exerts a substantial influence on the shape of the interaction potential.

Of direct relevance to maser formation, larger differences between λ-doublet populations are indeed observed. The authors argue that physically, the unpaired electron should tend to be oriented toward the H_2 and thus form a weak bond in the collision complex, which is calculated to be planar at the equilibrium geometry [150, 151]. Thus one expects that the OH, and hence the unpaired electron, will rotate preferentially in that plane. Because the energetic ordering of λ-doublet levels is reversed between the two spin–orbit manifolds, this mechanism favours the lower λ-doublet level in the $^2\Pi_{3/2}$ spin–orbit state, and the upper level in the $^2\Pi_{1/2}$ state. This is precisely the observed trend. In the $^2\Pi_{3/2}$ manifold, the collision cross-sections are larger for the lower-energy λ-doublet states, implying anti-inversion and ruling out the possibility that H_2 collisions lead to maser action. Population inversion is observed, however, for $j_f = 2{\cdot}5$, $3{\cdot}5$, and $4{\cdot}5$ in the $^2\Pi_{1/2}$ manifold, though not $j = 0{\cdot}5$. Furthermore, it is calculated that radiative relaxation of these inverted levels to the ground state can, in fact, result in a $\sim 20\%$ net inversion of $OH(X^2\Pi_{1/2}, j = 0{\cdot}5)$; this mechanism may be responsible for the astronomical OH maser in this state.

Sonnenfroh *et al.* [152] have used a similar technique to study inelastic scattering in the potentially reactive systems $OH(X^2\Pi_{3/2}, n = 0) + CO$, and $OH(X^2\Pi_{3/2}, n = 0) + N_2$, the latter of which samples the exit channel of the chemical reaction of H with N_2O. The integral cross-sections, summed over λ-doublet and spin–orbit states, drop off steadily with increasing n_f. Interestingly, rotational states are not populated up to the energetic limit. The authors ascribe this feature to weak anisotropy of the $OH + N_2$ and $OH + CO$ potentials, so that insufficient torque exists to induce very large changes in j. For both collisions systems, the ratio of spin–orbit conserving to spin–orbit changing cross-sections declines steadily from ~ 3, for $n = 2$, to $\leqslant 2$ for $n = 4$. Although a simple physical picture is not evident, this result can be understood theoretically by appealing to the two potential energy surfaces A' and A'', which differ with respect to the orientation of the unpaired electron

orbital. The matrix elements for the collision interaction are related to the average and difference potentials V^+ and V^-, given by [51, 149, 153–157]

$$\left.\begin{aligned} V^+ &= 1/2(V_{A'} + V_{A''}), \\ V^- &= 1/2(V_{A'} - V_{A''}). \end{aligned}\right\} \tag{9}$$

For a Hund's case (*a*) molecule, such as OH in low rotational states, spin–orbit conserving collisions are governed by V^+, and spin–orbit changing collisions by V^-. Thus the tendency to preserve a spin–orbit state at low n ($n = 2$) indicates a dominance of the sum potential V^+, providing a direct test of theoretical potential energy surfaces. At higher n ($n = 4$), spin-uncoupling in OH leads to mixing of the spin–orbit states (Hund's case (*b*)), which in turn means that both V^+ and V^- contribute to collisions within and between the spin–orbit manifolds. Therefore the spin–orbit populations are expected to equilibrate for higher rotational states, as observed.

The ratio of population in e/f λ-doublet levels, for $OH(n_i = 0) + CO$, is approximately independent of n_f. Interestingly, however, for $OH + N_2$ this ratio is ~ 1 for $n_f = 2$, but increases steadily with increasing n_f. The authors point out that a λ-doublet preference results from interfering partial waves scattering from V^+ and V^-. From *ab initio* calculations of the OH + CO potentials, it is known that at long range V^+ and V^- have opposite signs almost everywhere; for small distances where repulsive forces dominate, the ordering reverses. This change in sign may tend to cancel any preference for one or the other λ-doublet state in OH + CO. Once again the shape of the intermolecular potential energy surface, and not energetic or angular momentum constraints on the rotationally inelastic collision, dictate the energy transfer dynamics.

In related work, Macdonald and Liu have measured integral cross-sections for $CH(X^2\Pi) + He$ [158] and D_2 [159]. In these studies, the integral cross-sections were measure as a function of collision energy, which was varied from $\sim$ 20–200 meV by changing the angle at which the beams intersected. Because the A' and A'' surfaces for CH + He are both repulsive, whereas a deep well exists in the A' potential for $CH + D_2$, comparison of CH energy transfer with these equally massive gases allows one to separate kinematic and dynamical effects in the energy transfer process. In addition, except at very low j, CH is well described as a Hund's case (*b*) radical [49], and is thus a prototype for energy transfer in a spin-uncoupled free radical. In a collision with a Hund's case (*a*) radical, it can be shown that both magnitude of the nuclear rotation, and the sign of the orbital angular momentum, must be changed to alter the spin–orbit state. In a Hund's case (*b*) radical such as CH, a change in the magnitude of the nuclear rotation alone can cause a switch from one spin–orbit state to the other. One might anticipate, therefore, quite different collision dynamics for radicals with different degrees of spin-uncoupling.

For both collider gases He and D_2, the values $\sigma_{i \to f}$, summed over all spin–orbit and λ-doublet states, decrease monotonically with increasing n_f regardless of E_{coll}. From extensive measurements on $CH(n_f = 5)$ and as verified by spot checks on other levels, interesting dependencies are observed among the fine structure states as the collision energy is varied. The spin–orbit states for a given n_f are formed with a slight preference for the higher energy spin–orbit manifold.

More strikingly, a preference is observed to form λ-doublet states with the orbital of the unpaired electron out of the plane of rotation. For both spin–orbit states, the ratio of populations for out-of-plane against in-plane rotation exhibits a dramatic dependence on collision energy, and is highest near the energetic threshold for a given rotational

level. The physical origin of this effect reflects interferences among partial waves scattering from the average and difference potentials of equation (9). Since the deep well in the CH + D_2 A'' surface should result in a large difference potential V^-, it might be anticipated that the alignment would be more pronounced for D_2 that for He. Interestingly, the opposite ordering is observed. The authors have postulated that in CH + D_2, collisions that sample the attractive well are likely to react and form CD + HD, and thus contribute little to the observed CH alignment. In this case, the λ-doublet propensities are controlled by the repulsive portions of the potential, where the chemically reactive intermediate is not formed. Alexander and Dagdigian [160] have shown that such λ-doublet preferences can be explained by a curve crossing process, in which the CH enters on the A' surface for a given n, but crosses over to the A'' potential for $n-1$. For the CH + Ar test system, this curve crossing occurs only for a 'helicopter' approach in which the CH rotates in a plane perpendicular to the collision velocity. In short, the simple observation of λ-doublet propensities in Hund's case (b), $^2\Pi$ radicals can provide surprisingly detailed information regarding the collision dynamics and the shape of the intermolecular potentials.

Of great dynamical interest is the possibility of rotational rainbows, which result from interfering trajectories as a function of impact parameter and orientation of the CH with respect to the collider gas. Although it might be supposed that the existence of such rotational rainbows would be manifested most obviously as angular peaks in the *differential* cross-section, Schinke [161] has shown that characteristic effects can appear in the energy-dependent, integral cross-sections as well. Based on an impulsive, hard-shell model of the interaction potential, it is predicted that as E_{coll} is varied, rotationally excited products for a given n_f will not appear at their energetic threshold. Instead, their energetic onset will be higher by a value $\Delta E_{threshold}$, denoted a 'dynamical threshold', which is calculated to scale as n_f^2. In addition, each state-to-state, integral cross-section is expected to reach a maximum value as a function of collision energy at a value E_{max}, which also scales as n_f^2. In the CH + He scattering experiments, substantial dynamical thresholds are indeed observed. A plot of $\Delta E_{threshold}$ against n_f does show the expected quadratic behaviour for $n_f \leqslant 8$, suggesting the existence of rotational rainbow scattering. Furthermore, at $E_{coll} = 0{\cdot}17$ eV a semi-logarithmic plot of $\sigma_{i \to f}$ against n_f shows two linear decay regimes, intersecting at $n_f \sim 6$, a feature that is also well predicted by this theory. These indications are not conclusive, however; E_{max} scales linearly with n_f, and not quadratically as predicted. Still, the cross-sections show very broad maxima as a function of collision energy, which makes determination of E_{max} subject to a substantial uncertainty. Overall the evidence for rotational rainbow behaviour is compelling, and can provide a stringent test of theoretical potential energy surfaces. Clearly, it would be interesting to measure the differential cross-sections, to check for the anticipated rainbow maxima in $d\sigma/d\Omega$.

The hard-shell theory of Schinke applies to atom–diatom collision pairs, and thus might not necessarily be extrapolated to CH + D_2. In fact, averaging of all possible orientations of the two rotors could lead to quite different scattering dynamics, perhaps washing out any rainbow interference structure. Somewhat surprisingly, evidence for rotational rainbows nonetheless appears in the CH + D_2 data. Here again, dynamical thresholds are observed and scale quadratically with n_f. Also as observed for He, a semi-logarthmic plot of the integral cross-section against n_f shows two linear regions. However, the point at which these lines intersect is not at $n_f \sim 6$, as one predicts, but rather at $n_f \sim 4$, implying a different physical origin from that for CH + He. The authors note that CH($n = 4$) is quite close in its classical rotor frequency to that of $D_2(j = 2)$.

A plausible explanation is that the CH is first excited to $n_f = 6$, but subsequently suffers a secondary collision with the receding D_2 to give up two quanta of rotation. In other words, this unique collision results in frequency locking of the CH and D_2 collision partners.

The effects of two Renner–Teller potential energy (A'' and A') on the collision dynamics can be quite distinctive, as demonstrated cleanly in the studies of $NCO(X^2\Pi_{3/2}, n = 0) + He$ by Macdonald and Liu [162, 163]. In this work, the state-to-state, integral cross-sections decrease monotonically with increasing n_f for collisions that conserve the spin–orbit state. In marked contrast, the cross-sections for spin–orbit-changing collisions form a broad, bell-shaped curve, with a maximum at $n_f \sim 20$. To explain this, it is argued that the difference potential has the largest magnitude at close range, in the region of the van der Waals well. Therefore, changes in spin–orbit state are dominated by short-range collisions, which inherently sample small impact parameters. Because large impact parameters favour production of small Δn, collisions that change the spin–orbit state inherently favour larger changes in rotation, while suppressing the cross-sections at small n_f.

If a molecule with an unpaired electron collides with a closed shell species, the electron spin will not be flipped. However, if both collision partners have non–zero electron spin, the collision dynamics can change distinctly. Corey, Alexander, and Dagdigian [24] used a unique 'beam-gas' apparatus to measure integral cross-sections in $CaCl(X^2\Sigma^+) + NO(X^2\Pi)$, in which an electric quadrupole field was used to select a single j, m_j in a CaCl beam, which subsequently scatters over a short path length of a static, thermal, NO. The target beam was interrogated via LIF, at a short distance downstream of the entrance to the gas cell. The integral cross-sections were inferred from the j_f-dependent signal strengths, assuming isotropic m_j distributions and a predominantly forward-scattered (in the lab frame) CaCl. The authors have shown theoretically that in a collision, spin-correlation between a $^{2s+1}\Sigma$ target molecule (e.g., CaCl) and an open shell collider can lead to a reorientation of the electron spin. In this case the e and f symmetry labels distinguish the relative orientation of the electron spin and the nuclear rotation; a flip of the electron spin can cause $e \leftrightarrow f$ transitions. Nonetheless, a propensity was observed to *preserve* the *e/f* state of the CaCl. If long-range collisions dominate, the interaction of the two electrons is negligible and this result is not surprising. However, scattering calculations indicate that short-range collisions are in fact important. This implies that the CaCl–NO potential energy surfaces are largely unaffected by the presence of the unpaired spin, a reasonable conclusion since bond formation seems unlikely in the collision complex.

Recently, Schreel *et al.* [164], have implemented a highly state-selective, crossed beam experiment in which a single λ-doublet level in $OH(X^2\Pi_{3/2}, n = 0)$ is selected in a hexapole field, and collided with a beam of He or Ar; the state-to-state cross-sections for rotational energy transfer were measured using LIF. With Ar, energy transfer is dominated by $\Delta j = 0, 1$ within the $\Omega = 3/2$ spin–orbit state, implying that the average potential V^+ dominates the scattering. In contrast, for OH + He the cross-sections for spin–orbit changing/preserving collisions are quite similar. In general, for scattering of OH + He and Ar the cross-sections are larger for $f \rightarrow e$ transitions than for $f \rightarrow f$, although a few exceptions are noted. On the other hand, for scattering from the λ-doublet state of e symmetry into $j = 3/2, 5/2$ ($\Omega = 3/2$), $e \rightarrow e$ transitions are clearly favoured over $e \rightarrow f$. The integral cross-sections have been compared with the results of scattering calculations, on an *ab inito* potential of Werner; the overall agreement between experiment and theory is quite good.

Molecular beam studies of integral cross-sections for rotational energy transfer in free radicals have contributed substantially to the understanding of interaction potentials. Measurements of energy transfer propensities in and between the spin–orbit manifolds, in Hund's case (*a*) molecules, can provide direct probes of the Renner–Teller surfaces at long and short range. Similarly, the cross-sections for energy transfer among λ-doublet levels can reveal preferred orientations for the unpaired electron, and thus a preference for interaction on the A'' or A' Renner–Teller surface. Simple, purely repulsive models of the interaction potential can predict rainbow structure in the integral cross-sections for simple cases; conversely, unique dynamical behaviour such as frequency locking (for near-resonant states) can be revealed by the failure of such simple models to reproduce the j-dependent, integral cross-sections.

5.5. *Differential cross-section measurements*

As more detailed measurements of rotational energy transfer have arisen the desire for more thorough, theoretical understandings has naturally arisen. There has been a steady interest in the symbiotic development of high-resolution measurements with theoretical potential energy surfaces, to provide a theoretical framework. Since interfering trajectories on the interaction potentials can be manifested quite distinctly by rainbow scattering and diffraction oscillations, there has been a great deal of interest in measurements of *differential* cross-section measurements with which to test theory.

Pritchard and coworkers [165–167] have used laser Dopplerimetry, in a crossed molecular beam apparatus, to measure differential cross-sections for vibrationally and rotationally inelastic collisions in $Na_2(v = 0, j_i = 7) + Ar$. In these experiments, the Na_2 was probed as a function of j_f and velocity subgroup with a narrow band, c.w. dye laser before interaction with an Ar collider beam. The population of $Na_2(v_f, j_f \leqslant 80)$ was phase sensitively detected at the chopping frequency to provide a measure of the difference in population due to rotational energy transfer from the optically prepared state. The differential cross-sections, $d\sigma/d\Omega$, for all but the highest j_f exhibit an intense peak whose position moves to larger angles with increasing Δj. These maxima are attributed to rotational rainbow scattering or 'rotational halos' as preferred by the authors. The positions of the rainbow peaks are not significantly different for $\Delta v = 1$ than for $\Delta v = 0$, indicating that the vibrational dynamics do not significantly influence the rotational energy process. This is a somewhat surprising result because, as mentioned above, vibrationally inelastic energy transfer typically involves a hard, small impact parameter collision and thus samples a limited region of the intermolecular potential. In any event, according to a simple rigid ellipse model the position of the rainbow maximum θ_{max} should scale linearly with Δj, an observation that is verified experimentally. Moskowitz *et al.* [167] have shown that the slope of the best fit line through a plot of θ_{max} against Δj can be used to determine the difference r_m between the major and minor axes of the ellipse, providing a measure of the anisotropy of the potential in a simple, purely repulsive model.

Bergmann and coworkers [115, 168, 169] have also performed a series of measurements of rotationally inelastic scattering in $Na_2 + He$, Ne. Here the $Na_2(2 \leqslant j_i \leqslant 20)$ was optically pumped with an intensity-modulated laser; the population of $Na_2(j_f = 28)$ was probed as a function of scattering angle with a fibre-optic-coupled, rotatable LIF detector [115]. In interesting contrast with the above results for $Na_2 + Ar$, on average larger Δj transitions are observed for simultaneous changes in vibrational state. At fixed laboratory angles, the scattering cross-sections

exhibit steep shoulders as a function of Δj, again indicative of rainbow scattering (figure 7). At large centre-of-mass angles, the inelastic scattering processes are dominant. Since the Na_2 + He or Ne surfaces are unlikely to be characterized by deep attractive wells, rotationally inelastic energy transfer is most likely caused by small impact parameter collisions, thus favouring wide angle scattering as observed. As a function of laboratory angle, oscillatory structure is observed and attributed to rotational rainbows. This effect is most strikingly observed for $j_f = 0$, where supernumerary rainbow structure is clearly in evidence for Na_2 + He, Ne, and Ar [168]. From the positions of the maxima in these oscillations, the anisotropy parameter r_m from the rigid ellipse model can be determined; the value of r_m for Ar is quite close to that determined by Pritchard and coworkers [167] (see above). In collisions of vibrationally excited $Na_2(v = 31)$ + Ne, the value of r_m indicates a more anisotropic surface than is determined for $Na_2(v = 0)$ + Ne. Since the increased anisotropy implies that weaker collisions, or larger impact parameter collisions, can lead to large Δj, the differential cross-sections are expected and observed to shift to smaller scattering angles.

Buck and coworkers [107, 170–173] have used time-of-flight mass spectrometry to perform early differential cross-section measurements in HD and D_2. By virtue of large rotational constants, these molecules can be detected with rotational state resolution, allowing a detailed comparison of experimental and theoretical results (figure 8). Particular emphasis was placed on HD, D_2 + Ne, with an eye toward empirical refinement of an H_2 + Ne potential energy surface as a function of radial distance r, and angle γ with respect to the bond axis, $HD(j_f = 1)$ and $D_2(j_f = 2)$ were observed, as were the elastic ($j_i = j_f$) channels, with well resolved diffraction oscillations in $d\sigma/d\Omega$. The intermolecular potential was approximated by a Legendere polynomial series truncated at the lowest anisotropic term,

$$V(r, \gamma) = V_0(r) = V_2(r)P_2(\cos\gamma). \tag{10}$$

For D_2 + Ne, the authors have shown that if (i) only $j = 0, 2$ are populated, (ii) the orbital angular momentum is essentially unchanged in the collision, and (iii) inelastic collisions only occur for large-angle scattering (i.e., small impact parameters), then using a classical correspondence between orbital angular momentum and scattering angle, the differential cross-section data can be inverted directly to determine $V_0(r)$ and $V_2(r, \gamma)$. The resulting potential gives reasonable agreement with the observed data beyond the region of large diffraction oscillations. Because of the classical approximations involved, however, the oscillatory structure in $d\sigma/d\Omega$ is not accurately reproduced.

When higher-order terms are included in (10), the radial functions $V_n(\cos\gamma)$ no longer bear a unique mathematical relationship to the scattering cross-sections. Iterative determination of such a potential, based on a least squares fit to the observed differential cross-sections, is possible in principle but computationally prohibitive. Furthermore, for molecule–molecule scattering the potentials reflect more degrees of freedom, exponentially increasing the size of the scattering matrix. It is useful, then, to determine which regions of the potential are most critical in determination of $d\sigma/d\Omega$. In subsequent work on HD + D_2 Buck *et al.* [107]. have shown that, for a collision wave-number (i.e., inverse De Broglie wavelength) κ and impact parameter b, the angular spacing $\Delta\theta$ between successive peaks in the elastic, diffraction oscillations is approximately given by

$$\Delta\theta = \pi/\kappa b. \tag{11}$$

Furthermore, the slopes of the isotropoic term can be obtained from the ratio of the integral cross-sections for HD, $\sigma_{0\to1}/\sigma_{0\to0}$, that is, the inelastic to elastic scattering cross-sections. From such an analysis, the *ab initio* potential of Meyer and Schaefer [174] has been empirically modified; the resulting differential cross-sections, calculated on the new surface, reproduce the observed cross-sections within experimental uncertainties. Faubel *et al.* have recently used differential scattering measurements for H_2 + F[175] to construct simple, model potentials for this system; the data were found to be equally well represented by more than one potential energy surface, suggesting that more detailed modelling is required.

The first scattering measurements for the spherical top CH_4 + He, Ne, and Ar were performed by Buck and coworkers [127–129, 176, 177] in a similar experimental arrangement. For CH_4 + He, the final states j_f are partially resolved in the time-of-flight mass spectrometer, enabling the extraction of state-to-state cross-sections for some j_f. For Ne and Ar, the final states overlap considerably; nonetheless, distinct oscillations in the total, differential cross-section are evident. For He, the scattering at low j_f is predominantly into small angles in the centre of mass frame, i.e. is mostly in the forward

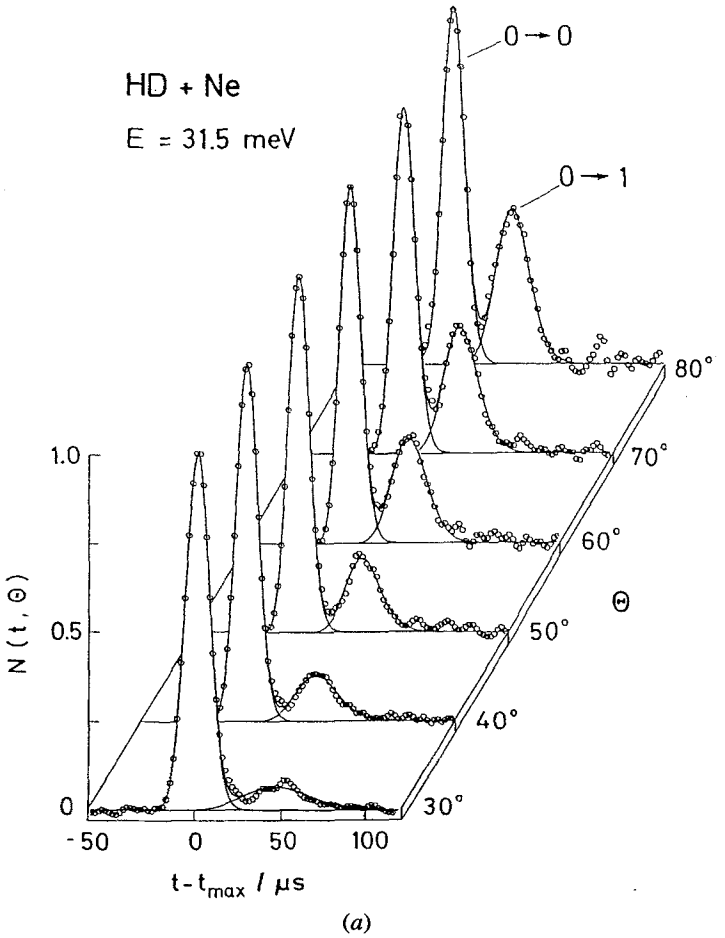

(*a*)

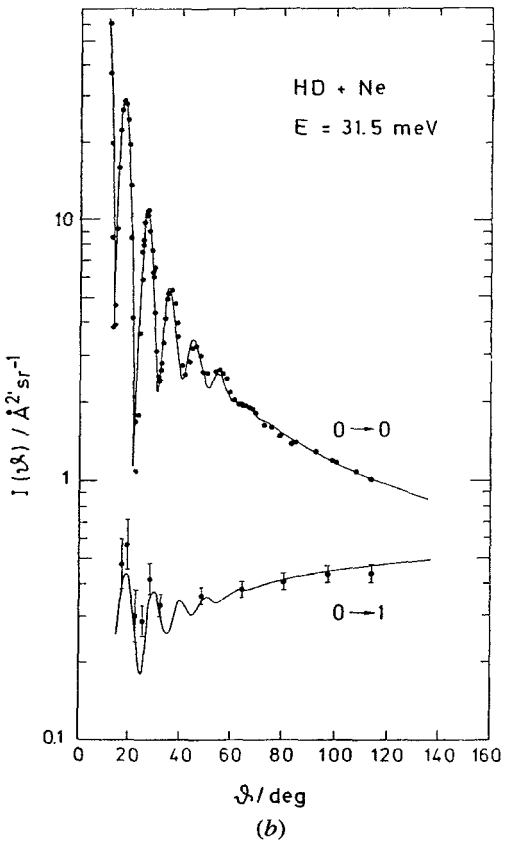

(*b*)

Figure 8. Time-of-flight, mass spectra of HD scattered from Ne in crossed molecular beams, as a function of laboratory angle (from [170]). From energy conservation in the T–R collision process, the time-of-flight spectrum can be mapped onto an energy loss spectrum; the peaks in the time domain correspond to HD($j_f = 0$) and HD($j_f = 1$). From these data, the state-to-state, differential cross-section can be determined. (*b*) Differential cross-section for elastic and inelastic scattering channels in HD + Ne (from [173]). The intermolecular potential can be determined, to lowest order in the angular anisotropy, from the positions of the well-resolved diffraction oscillations.

direction. As j_f increases, side- and eventually back-scattering is observed. Such a trend, from forward to back scattering as the rotational inelasticity is increased, can be predicted qualitatively by a simple, repulsive ellipsoid model of the potential energy surface. At a more detailed level, Malik, *et al.* [176] have performed scattering calculations on model potential energy surfaces for CH_4 + Ar, and have made similar predictions for widely varying strengths of the attractive and repulsive anisotropies in the CH_4 + Ar potential. More recently, Chapman *et al.* [126] have used infrared Dopplerimetry to determine, with low angular resolution, the CH_4 + He, Ne, and Ar differential cross-sections and have found that the scattering is predominately in the forward direction at low j_f, but becomes increasingly side scattered for higher j_f up to 6. In conjunction with these experiments, a great deal of effort has gone into development of *ab initio* and empirical potential energy surfaces. Despite the remarkable angular resolution of the total, differential cross-sections as determined with

the time-of-flight technique, determinations of the angular anisotropy for these potentials have been possible only to the lowest order of an expansion in spherical tensor operators. Higher terms are surprisingly insensitive to shape of $d\sigma/d\Omega$. In conjunction with the state-to-state, *integral* cross-section measurements of Schiffman *et al.* [125] and Chapman *et al.* [126], however, more exact determinations of these surfaces seems possible.

An unusual observation has been made by Buck *et al.* in the scattering of CO_2 + Xe [28, 29]. At a small centre-of-mass scattering angle, the time-of -flight mass spectrum is characterized by a single, broad peak at small ΔE. At larger angles, this peak broadens further and then splits in two, with maxima at small and large values of the fractional energy loss. These peaks do not occur at the correct energies to correspond to vibrational excitation of the CO_2 bend. Moreover, if the structure is a rotational rainbow effect, one expects (from a rigid ellipsoid model) the peak at large ΔE to increase with increasing angle, yet precisely the opposite trend is observed. To investigate the origin of these mysterious observations, the authors have carried out both quantum close-coupling and classical trajectory calculations on a model surface, treating the CO_2 as a rigid rotor. Examination of the *classical* trajectories that scatter into intermediate angles reveals that the classical angular momentum almost reaches the maximum allowed value during the collision, leaving the colliding fragments with little remaining translational energy. As the CO_2 and Xe fly apart, the CO_2 angular momentum decreases to its final value. Thus it appears that during the collision the slow-moving Xe, caught in the vicinity of the rapidly rotating CO_2, undergoes a *secondary* collision with the CO_2 and reduces its angular momentum. This dynamic is manifested as the observed, angle-dependent peak in the energy loss spectrum, termed a 'multiple-collision rotational rainbow'.

A novel ion imaging [178, 179] approach to the determination of state resolved, differential cross-sections has been applied to $NO(^2\Pi_{1/2}, v = 0, n = 0)$ + Ar by Suits *et al.* [180] and Bontuyan *et al.* [181]. In this crossed molecular beam experiment, rotationally excited $NO(v = 0, j_f)$ is state selectively ionized with a pulsed laser in the molecular beam intersection region, and extracted into a Wiley–Mclarin mass spectrometer, oriented perpendicular to the collision plane. The ion cloud is accelerated onto a microchannel plate/phosphor assembly, creating a two-dimensional projection of the NO Newton sphere; the image from the phosphor screen is recorded with a charge-coupled device (CCD) camera. The result is a spatial image of the differential cross-section for $NO(j_f)$, projected onto a plane (figure 9). The three-dimensional differential cross-section can then be extracted by a forward convolution model that assumes a differential cross-section, and accounts for spatial blurring due to finite molecular beam sizes, non-symmetry of the recorded images, etc.

Because spin–orbit changing/preserving collisions in a Hund's case (*a*) molecule are driven independently by the difference/sum potentials, V^- and V^+, one might suppose that the differential cross-sections would be quite different. The structure of the differential cross-section for a given j_f, however, is largely unchanged for collisions that preserve against alter the spin–orbit state. In addition, the integral cross-sections for multiplet-changing collisions *increase* with increasing Δj. One possible explanation is that, at the highest observed j_f, spin uncoupling is significant and NO is best described with an admixture of Hund's case (*a*) wavefunctions. This mixing is stronger for higher j_f, which would account for the rising trend in the integral cross-sections for multiplet-changing collisions.

At high j_f distinct peaks are observed in $d\sigma/d\Omega$, attributed to rotational rainbow scattering. The rainbow maxima shift to increasing back-scattered angles, in the centre-

of-mass frame, as j_f increases. Furthermore, at high j_f *two* rainbow peaks appear. The double rainbow arises from scattering interferences from both ends of the NO molecule, and represents the first such direct observation. As the collision energy is increased, the rainbow angle moves to smaller scattering angles, presumably because the higher collision energy results in less efficient momentum transfer and hence smaller deflection angles.

In summary, measurements of differential cross-sections for rotational energy transfer reveal detailed dynamics of the collision process, and have been particularly instrumental in testing the predictive accuracy of classical and *ab initio* potential energy surfaces. As a general trend, and remarkably independent of the form of the interaction potential, provided that collisions are largely impulsive, the differential cross-sections are often dominated by forward scattering for collisions with small rotational inelasticities. As Δj is increased, side- and eventually back-scattered angles are increasingly sampled in the centre of mass frame. Such a general trend is predicted qualitatively by repulsive, hard ellipse models. From the spacings of observed diffraction oscillations, the major and minor axes characterizing this ellipse can be determined; therefore, the differential cross-sections quite directly reflect an approximate, repulsive, angular anisotropy of the potential. Complex formation and multiple, collisional encounters can be inferred from the structure of the cross-sections. From a combination of differential cross-section measurements, and state-resolved, integral; cross-section measurements, the goal of accurate determination of intermolecular potentials from scattering data is becoming increasingly feasible.

5.6. mj-*changing collisions*

An intriguing result of the HF + Ar studies of Polanyi [119] mentioned earlier is that the empirically determined rate constants for upward against downward Δj do not satisfy microscopic reversibility. The authors argue that the j-dependent, spectral intensities could be qualitatively explained by a persistent, non-uniform m_j distribution.

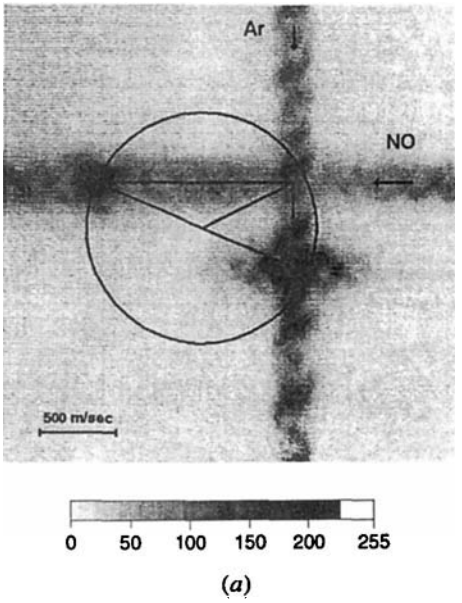

(*a*)

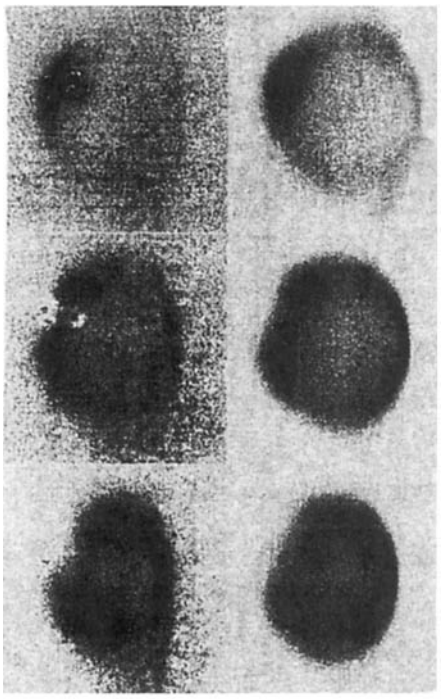

(*b*)

Figure 9. Ion imaging of NO + Ar in crossed, molecular beams (see [180, 181] for similar figures). (*a*) Superimposed images of the nascent target and collider beams. The dark spots are the Ar and NO, ionized at the beam intersection and spatially displaced during their flight times in the mass spectrometer. The Newton diagram for the elastic scattering channel is also shown. (*b*) Angular distributions for NO($j_f = 7{\cdot}5$) at $E_{coll} = 0{\cdot}18$ eV. The column on the left shows unprocessed ion images for (top to bottom) $j_f = 7{\cdot}5$, $11{\cdot}5$, $18{\cdot}5$ ($\Omega = 1/2$ spin–orbit state), representing projections of the Newton spheres onto two dimensions. On the right are the simulated images using a Monte Carlo, forward convolution technique. The extent to which they match the data indicates how well the differential cross-sections are chosen.

The non-random population of magnetic sublevels in turn could be produced by the polarized excitation laser; this cannot be the whole explanation, however, since rotation of the electric field of the HF laser by 90° produced no significant change in the observed signals. An alternative possibility is alignment of the HF from directed collisions in the nascent supersonic expansion, as has been observed more recently for CO_2 [182]. Regardless of the mechanism, the data provide strong evidence that for a diatomic target molecule and an atomic collider, m_j is not readily changed in a collision, a result consistent with the thermal cell studies mentioned above. In the thermal cell studies in which m_j-changing collisions were studied, only the lowest non-zero moments of the m_j distribution could be determined; a propensity for $\Delta m_j \ll j$ is consistent with the data, but not unambiguously demonstrated. The evidence is strong, however, and has invited more fully state-resolved studies.

Khare *et al.* [183] have suggested that the selection rule $\Delta m = 0$ should apply with respect to the direction along which linear momentum is transferred, denoted the 'kinematic apse'. The physical basis is simple: in order to conserve angular momentum,

any change in **j** must be perpendicular to the change in linear momentum $\Delta\mathbf{p}$. Consequently, the projection of **j** and **p** cannot change, and $\Delta m = 0$. To test this hypothesis, Mattheus *et al.* [184] have used linearly polarized light to saturate a transition in a beam of $Na_2(j_i \neq 0)$, thereby preparing a highly aligned sample with respect to the electric field vector of the laser, $\boldsymbol{\varepsilon}$. The alignment of the Na_2 with respect to $\Delta\mathbf{p}$ can be determined by a straightforward transformation. The Na_2 was scattered out of the target beam by a collider beam of Ne. The population of $Na_2(j_f = 0)$ was detected, at a fixed laboratory angle and at a large distance from the scattering centre using LIF. The direction of $\boldsymbol{\varepsilon}$ was rotated in the collision plane, and the LIF intensity measured as a function of this rotation angle, and of the P, Q, or R pump transition. The resulting LIF intensities for $j_i = 6$ are well modelled assuming that $\Delta m = 0$. Less than 50% of the collisions are estimated to proceed with $\Delta m > 0$. This represents a direct, experimental demonstration that $\Delta m \ll j_i$.

6. Concluding remarks

The study of rotational energy transfer has spanned many decades, and for many systems has led to an increasingly detailed understanding of the underlying dynamics, and to some extent the features of intermolecular potentials. From the earliest studies in thermal cells, the importance of multi-quantum transfers was evident even in systems that involve strong dipole–dipole interactions. Simple energy gap and momentum gap formulae can account for the shape of the energy transfer function for a number of collision systems; such empirical laws are of value for parameterizing large amounts of data, but show little promise for predicting the behaviour of unstudied systems. Indeed, even the premise of a monotonic decrease in the state-to-state cross-sections, upon which such formulations are based, is routinely violated.

The state-to-state rate for rotationally inelastic energy transfer are typically quite large (on the order of gas kinetic) unless the energy spacings greatly exceed kT. These rates can be enhanced by long-range attractive forces or, for molecular colliders, by near-resonant energy transfer into internal modes of both colliding species. Furthermore, the propensities for scattering into a given set of final j states can be greatly influenced by complex formation, simultaneous vibrational and rotational transfer, multiple encounters during a collision, tendency to preserve electron spin, and symmetry of the molecule. For most atom–molecule systems, the number of populated j_f states tends to increase with increasing mass of the atom, as a consequence of the increased orbital angular momentum available for a given collision energy and impact parameter; at sufficiently high j_i, however, rotational averaging of the intermolecular potential can give an effectively more isotropic interaction, leading to inefficient energy transfer.

In $^1\Pi$ molecules, dependencies of the state-to-state rate constants on the λ-doublet level can be important, and can provide signatures of the favoured directions of approach with respect to the unpaired electron orbital. The j- and λ-doublet-dependent cross-sections are determined by interferences on the two (A' and A'') intermolecular potential energy surfaces that drive the collisional exchange of energy, and hence are not predictable from classical reasoning. Complex formation appears to facilitate both rotational and λ-doublet changing collisions. These dynamics can account for the λ-doublet specificity that is often observed, and can account for non-equilibrium state distributions, in particular for the collisional formation of interstellar masers. In $^2\Pi$ molecules, spin–orbit changing collisions can also be greatly accelerated by the formation of stable complexes. In these free radicals, the operation of two

(Renner–Teller) potential energy surfaces can lead to interfering trajectories that are manifested in the propensities to preserved or change the spin–orbit state; stated conversely, studies of spin–orbit energy transfer can provide a unique probe for the intermolecular potential energy surfaces.

Collisions that re-orient m_j are generally found to proceed inefficiently with respect to those for j-changing collisions. In fact, non-equilibrium (oriented or aligned) m_j distributions can remain remarkably undisturbed over numerous hard-sphere collisions. The amount of data is too sparse and inconclusive to make firm statements about the shape of the m_j transfer function. Some data indicate an apparent m_j conservation, while other studies suggest that the orientation of the **j** vector is the preserved quantity in a collision. Further experiments seem warranted in this area.

The study of rotational energy transfer of polyatomic species shows specificity in the energy transfer on vibrational level, parity, K quantum number and symmetry. Strong selectivity in symmetric and spherical top molecules, due purely to their symmetry, is both observed experimentally and predicted theoretically; in such systems, rotational energy transfer can not be described by energy or angular momentum gap models. A relatively untrodden field is that of state-resolved energy transfer in polyatomic molecules at high, chemically interesting levels of rovibrational excitation, where the density of states can be quite high. Such studies, which sample intermolecular potentials in regions that approach the transition states, have only begun to provide a link between reactive and inelastic scattering processes.

An active area of research has been the accurate determination of intermolecular potentials from state-resolved scattering data. This task is generally involved computationally and difficult experimentally, and has been carried out for relatively few systems. Because scattering interferences can produce distinct oscillations in the differential cross-section, the high angular resolution afforded in many crossed beam experiments has been an important bridge between experiment and theory. Unfortunately, few studies currently exist in which *state-resolved* differential cross-sections are determined, although the amplitudes and spacings of the diffraction oscillations can be far more sensitive to the shape of the potential energy surface than are the *total* differential cross-sections. Of particular promise are the laser based methods for determination of integral and differential cross-sections. With such techniques, the empirical testing and refinement of potentials for an increasingly broad variety of collision systems appears to be on the horizon.

Acknowledgments

The authors would like to thank Dr M. H. Alexander and Dr P. J. Dagdigian for valuable discussions, and all who contributed figures. This work is supported by the U.S. Department of Energy, Office of Basic Energy Sciences, Division of Chemical Sciences.

References

[1] HIRSCHFELDER, J. O., CURTISS, C. F., and BIRD, R. B., 1954, *Molecular Theory of Gases and Liquids* (New York: Wiley).

[2] HERZFELD, K. F., and LITOVITZ, T. A., 1959, *Absorption and Dispersion of Ultrasonic Waves* (New York: Academic).

[3] BRASSEUR, G., and SOLOMON, S., 1986, *Aeronomy of the Middle Atmosphere* (Dordrecht: Reidel).

[4] RAO, K. N., 1972, *Molecular Spectroscopy: Modern Research* (New York: Academic).

[5] YELLE, R. V., 1991, *Asrophys. J.*, **383,** 380.

[6] SIRKIN, E. R., and PIMENTEL, G. C., 1981, *J. chem. Phys.*, **75,** 604.
[7] ONORATU, M., 1982, *Gas Flow and Chemical Lasers* (New York: Plenum).
[8] BERTOJO, M., CHEUNG, A. C., and TOWNES, C. H., 1976, *Astrophysics. J.*, **208,** 914.
[9] KOSLOFF, R., KAFRI, A., and LEVINE, R. D., 1977, *Astrophys. J.*, **215,** 497.
[10] GAYDON, A. G., 1974, *The Spectroscopy of Flames* (New York: Wiley).
[11] WEISSHAR, J. C., BAMFORD, D. J., SPECHT, E., and MOORE, C. B., 1981, *J. chem. Phys.*, **74,** 226.
[12] SCHIFFFMAN, A., and NESBITT, D. J., 1993, *J. chem. Phys.*, **100,** 2677.
[13] PINE, A. S., and LOONEY, J. P., 1987, *J. molec. Spectrosc.*, **122,** 41.
[14] KOSZYKOWSKI, M., FARROW, R. L., and PALMER, R. E., 1985, *Optics Lett.*, **10,** 478.
[15] RAHN, L., and PALMER, R. E., 1986, *J. opt. Soc.* B, **3,** 1164.
[16] WILLIAMS, S., ZARE, R. N., and RAHN, L. A., 1994, *J. chem. Phys.*, **101,** 1072.
[17] PENDLETON, W., JR., ESPY, P., BAKER, D., STEED, A., and FETROW, M., 1989, *J. Geophys. Res.*, **94,** 505.
[18] SMITH, D. R., BLUMBERG, W. A. M., NADILE, R. M., LIPSON, S. J., HUPPI, E. R., and WHEELER, N. B., 1992, *Geophys. res. Lett.*, **19,** 505.
[19] OKA, T., 1968, *J. chem. Phys.*, **49,** 3135.
[20] FOY, B., HETZLER, J., MILLOT, G., and STEINFELD, J. I., 1988, *J. chem. Phys.*, **86,** 6838.
[21] HETZLER, J., MILLOT, G., and STEINFELD, J. I., 1989, *J. chem. Phys.*, **90,** 5434.
[22] HETZLER, J., and STEINFELD, J. I., 1990, *J. chem. Phys.*, **92,** 7135.
[23] KLAASSEN, J. I., and STEINFELD, J. I., and ROCHE, C., 1994, *J. chem. Phys.*, **100,** 5519.
[24] COREY, G. C., ALEXANDER, M. H., and DAGDIGIAN, P. J., 1986, *J. chem. Phys.*, **84,** 1547.
[25] ALEXANDER, M. H., DAVIS, S. L., and DAGDIGIAN, P. J., 1985, *J. chem. Phys.*, **83,** 556.
[26] CHILD, M. S., 1974, *Molecular Collision Theory, Theoretical Chemistry*, edited by D. P. Craig and R. McWeeny (Academic: New York).
[27] SCOLES, G., editor, 1988, *Atomic and Molecular Beam Methods* (Oxford University Press).
[28] BUCK, U., HUISKEN, F., OTTEN, D., and SCHINKE, R., 1983, *Chem. Phys. Lett.*, **101,** 126.
[29] BUCK, U., OTTEN, D., SCHINKE, R., and POPPE, D., 1985, *J. chem. Phys.*, **82,** 202.
[30] LAWLEY, K. P., 1980, *Adv. chem. Phys.*, p. 421.
[31] YARDLEY, J. T., 1980, *Introduction to Molecular Energy Transfer* (New York: Academic).
[32] FRANCK, J., and WOOD, R. W., 1911, *Phil. Mag.*, **21,** 314.
[33] MCCOUBREY, J. C., and MCGRATH, W. D., 1957, *Quart. Rev.*, **11,** 87.
[34] CARRINGTON, T., 1959, *J. chem. Phys.*, **31,** 1418.
[35] BROIDA, H. P., and CARRINGTON, T., 1963, *J. chem. Phys.*, **38,** 136.
[36] STEINFELD, J. I., and KLEMPERER, W., 1965, *J. chem. Phys.*, **42,** 3475.
[37] BRUNNER, T. A., DRIVER, R. D., SMITH, N., and PRITCHARD, D. E., 1979, *J. chem. Phys.*, **70,** 4155.
[38] BRUNNER, T. A., DRIVER, R. D., SMITH, N., and PRITCHARD, D. E., 1978, *Phys. Rev. Lett.*, **41,** 856.
[39] WAINGER, M., AL-AGIL, I., BRUNNER, T. A., KARP, A. W., SMITH, N., and PRITCHARD, D. E., 1979, *J. chem. Phys.*, **71,** 1977.
[40] BRUNNER, T. A., SMITH, N., KARP, A. W., and PRITCHARD, D. E., 1981, *J. chem. Phys.*, **74,** 3324.
[41] MCCORMACK, J., MCCAFFERY, A. J., and ROWE, M. D., 1980, *Chem. Phys.*, **48,** 121.
[42] MCCORMACK, J., and MCCAFFERY, A. J., 1980, *Chem. Phys.*, **51,** 405.
[43] CAUGHEY, T. A., and CROSLEY, D. R., 1978, *J. chem. Phys.*, **69,** 3379.
[44] KATO, H., CLARK, R., and MCCAFFERY, A. J., 1976, *Molec. Phys.*, **31,** 943.
[45] CLARK, R., and MCCAFFERY, A. J., 1978, *Molec. Phys.*, **35,** 617.
[46] JEYES, S. R., MCCAFFERY, A. J., and ROWE, M. D., 1977, *Chem. Phys. Lett.*, **48,** 91.
[47] SMITH, N., BRUNNER, T. A., KARP, A. W., and PRITCHARD, D. E., 1979, *Phys. Rev. Lett.*, **43,** 693.
[48] SMITH, N., BRUNNER, T. A., and PRITCHARD, D. E., 1981, *J. chem. Phys.*, **74,** 467.
[49] HERZBERG, G., 1950, *Spectra of Diatomic Molecules* (New York: Van Nostrand).
[50] OTTINGER, C., VELASCO, R., and ZARE, R. N., 1970, *J. chem. Phys.*, **52,** 1636.
[51] LEMOINE, D., COREY, G. C., ALEXANDER, M. H., and DEROUARD, J., 1987, *Chem. Phys.*, **118,** 357.
[52] AL-IMARAH, F. J., BAIN, A. J., MEHDE, M. S., and MCCAFFERY, A. J., 1984, *J. chem. Phys.*, **82,** 1298.

[53] HUCKNALL, D. J., 1985, *Chemistry of Hydrocarbon Combustion* (New York: Chapman and Hall).
[54] LENGEL, R. K., and CROSLEY, D. R., 1977, *J. chem. Phys.*, **67,** 2085.
[55] BERRY, M. T., BRUSTEIN, M. R., ADAMO, J. R., and LESTER, M. I., 1988, *J. phys. Chem.*, **92,** 5551.
[56] BERRY, M. T., BRUSTEIN, M. R., and LESTER, M. I., 1988, *Chem. Phys. Lett.*, **153,** 17.
[57] BERRY, M. T., BRUSTEIN, M. R., and LESTER, M. I., 1989, *J. chem. Phys.*, **90,** 5878.
[58] BERRY, M. T., LOOMIS, R. A., GIANCARLO, L. C., and LESTER, M. I., 1992, *J. chem. Phys.*, **96,** 7890.
[59] FAWZY, W. M., and HEAVEN, M. C., 1988, *J. chem. Phys.*, **89,** 7030.
[60] JORG, A., MEIER, U., and KOHSE HOINGHAUS, K., 1990, *J. chem. Phys.*, **93,** 6453.
[61] DEGLI ESPOSTI, A., and WERNER, H.-J., 1990, *J. chem. Phys.*, **93,** 3351.
[62] JORG, A., DEGLI ESPOSTI, A., and WERNER, H.-J., 1990, *J. chem. Phys.*, **98,** 8757.
[63] DUFOUR, C., PINCHEMEL, B., DOUAY, M., SCHAMPS, J., and ALEXANDER, M. H., 1985, *Chem. Phys.*, **98,** 315.
[64] HERZBERG, G., 1966, *Electronic Spectra of Polyatomic Molecules* (New York: Van Nostrand).
[65] OKA, T., 1966, *J. chem. Phys.*, **45,** 752.
[66] GORDON, R. G., LARSON, P. E., THOMAS, C. H., and WILSON, E. B., 1969, *J. chem. Phys.*, **50,** 1388.
[67] TAATJES, C. A., and LEONE, S. R., 1988, *J. chem. Phys.*, **89,** 302.
[68] SCHWARTZ, R. N., SLAWSKY, Z. I., and HERZFELD, K. R., 1952, *J. chem. Phys.*, **20,** 1591.
[69] HINCHEN, J. J., and HOBBES, R. H., 1976, *J. chem. Phys.*, **65,** 2732.
[70] OKA, T., 1973, *Adv. atom molec. Phys.*, **9,** 127.
[71] COPELAND, R. A., and CRIM, F. F., 1983, *J. chem. Phys.*, **78,** 5551.
[72] COPELAND, R. A., and CRIM, F. F., 1984, *J. chem. Phys.*, **81,** 5819.
[73] MENARD-BOURCIN, F., DELAPORTE, T., and MENARD, J., 1986, *J. chem. Phys.*, **84,** 201.
[74] ROHLFING, E. A., CHANDLER, D. W., and PARKER, D., 1987, *J. chem. Phys.*, **87,** 5229.
[75] CHANDLER, D. W., and FARROW, R. L., 1986, *J. chem. Phys.*, **85,** 810.
[76] FARROW, R. L., and CHANDLER, D. W., 1988, *J. chem. Phys.*, **89,** 1994.
[77] SITZ, G. O., and FARROW, R. L., 1990, *J. chem. Phys.*, **93,** 7883.
[78] DEPRISTO, A. E., BELBRUNO, J. J., GELFLAND, J., and RABITZ, H., 1981, *J. chem. Phys.*, **74,** 5031.
[79] BONAMY, L., BONAMY, J., ROBERT, D., LAVOREL, B., SAINT-LOUP, R., CHAUX, R., SANTOS, J., and BERGER, H., 1988, *J. chem. Phys.*, **89,** 5568.
[80] PARSON, R., 1990, *J. chem. Phys.*, **93,** 8731.
[81] ORR, B. J., HAUB, J. G., and HAINES, R., 1984, *Chem. Phys. Lett.*, **107,** 169.
[82] ORR, B. J., HAUB, J. G., NUTT, G. F., STEWARD, J. L., and VOZZO, O., 1981, *Chem. Phys. Lett.*, **78,** 621.
[83] BEWICK, C. P., DUVAL, A. B., and ORR, B. J., 1985, *J. chem. Phys.*, **82,** 3471.
[84] BEWICK, C. P., HAUB, J. G., HYNES, R. G., MARTINS, J. F., and ORR, B. J., 1988, *J. chem. Phys.*, **88,** 6351.
[85] BEWICK, C. P., and ORR, B. J., 1989, *Chem. Phys. Lett.*, **159,** 73.
[86] LUTZ, A. L., TOBIASON, J. D., CARRASQUILLO, E., FRITZ, M. D., and CRIM, F. F., 1992, *J. chem. Phys.*, **97,** 389.
[87] TOBIASON, J. D., LUTZ, A. L., and CRIM, F. F., 1992, *J. chem. Phys.*, **97,** 7437.
[88] TEMPS, F., HALLE, S., VACCARO, P. H., FIELD, R. W., and KINSEY, J. L., 1987, *J. chem. Phys.*, **87,** 1895.
[89] TEMPS, F., HALLE, S., VACCARO, P. H., FIELD, R. W., and KINSEY, J. L, *J. chem. Soc., Faraday Trans.*, **84,** 1457.
[90] SITZ, G. O., and FARROW, R., 1994, *J. chem. Phys.*, **101,** 4682.
[91] SUDBØ, A. S., and LOY, M. M. T., 1982, *J. chem. Phys.*, **76,** 3646.
[92] LIN, S. H., FUJIMURA, Y., NEUSSER, H. J., and SCHLAG, E. W., 1984, *Multiphoton Spectroscopy of Molecules* (New York: Academic).
[93] YANG, X., and WODTKE, A. M., 1992, *J. chem. Phys.*, **96,** 5123.
[94] O'NEILL, J. A., WANG, C. X., CAI, J. Y., FLYNN, G. W., and WESTON, R. E., JR., 1986, *J. chem. Phys.*, **85,** 4195.

[95] HEWITT, S. A., HERSCHBERGER, J. F., FLYNN, G. W., and WESTON, R. E., JR., 1987, *J. chem. Phys.*, **87,** 1894.
[96] HERSHBERGER, J. F., HEWITT, S. A., FLYNN, G. W., and WESTON, R. E., JR., 1988, *J. chem. Phys.*, **88,** 7243.
[97] HERSHBERGER, J. F., HEWITT, S. A., SARKAR, S. K. FLYNN, G. W., and WESTON, R. E. JR., 1989, *J. chem. Phys.*, **91,** 4636.
[98] KREUTZ, T. G., KHAN, F. A., and FLYNN, G. W., 1990, *J. chem. Phys.*, **92,** 347.
[99] HEWITT, S. A., HERSHBERGER, J. F., CHOU, J. Z., FLYNN, G. W., and WESTON, R. E. JR., 1990, *J. chem. Phys.*, **93,** 4922.
[100] KREUTZ, T. G., and FLYNN, G. W., 1990, *J. chem. Phys.*, **93,** 452.
[101] KHAN, F. A., KREUTZ, T. G., O'NEILL, J. A., WANG, C. X., and WESTON, R. E., JR., 1990, *J. chem. Phys.*, **93,** 445.
[102] KHAN, F. A., KREUTZ, T. G., FLYNN, G. W., and WESTON, R. E., JR., 1990, *J. chem. Phys.*, **92,** 4876.
[103] KHAN, F. A., KREUTZ, T. G., FLYNN, G. W., and WESTON, R. E., JR., 1993, *J. chem. Phys.*, **98,** 4876.
[104] ZHAO, Z.-Q., CHAPMAN, W. B., and NESBITT, D. J., *J. chem. Phys.* (in press).
[105] LEVINE, R. D., and BERNSTEIN, R. B., 1987, *Molecular Reaction Dynamics and Chemical Reactivity* (Oxford University Press).
[106] BUCK, U., HUISKEN, F., SCHLEUSENER, J., and PAULY, H., 1977, *Phys. Rev. Lett.*, **38,** 680.
[107] BUCK, U., HUISKEN, F., and SCHLEUSENER, J., 1978, *J. chem. Phys.*, **68,** 5654.
[108] GENTRY, W. R., and GIESE, C. G., 1977, *J. chem. Phys.*, **67,** 5389.
[109] GENTRY, W. R., and GIESE, C. G., 1977, *Phys. Rev. Lett.*, **39,** 1259.
[110] FAUBEL, M., KOHL, K. H., TOENNIES, J. P., YANG, K. T., and YUNG, Y. Y., 1982, *Faraday Disc. Chem. Soc.*, **73,** 205.
[111] KINSEY, J. L., 1977, *J. chem. Phys.*, **66,** 2560.
[112] TAATJES, C. A., CLINE, J. I., and LEONE, S. R., 1990, *J. chem. Phys.*, **93,** 6554.
[113] SERRI, J. A., BECKER, C. H., ELBEL, M. B., KINSEY, J. L., MOSKOWITZ, W. P., and PRITCHARD, D. E., 1981, *J. chem. Phys.*, **74,** 5116.
[114] SERRI, J. A., KINSEY, J. L., and PRITCHARD, D. E., 1981, *J. chem. Phys.*, **75,** 663.
[115] BERGMANN, K., HEFTER, U., and WITT, J., 1980, *J. chem. Phys.*, **72,** 4777.
[116] VAN HULST, N. F., 1986, PhD Dissertation, University of Nijmegen.
[117] DING, A. M. G., and POLANYI, J. C., 1975, *Chem. Phys.*, **10,** 39.
[118] LANG, N. C., POLANYI, J. C., and WANNER, J., 1977, *Chem. Phys.*, **24,** 219.
[119] BARNES, J. A., KEIL, M., KUTINA, R. E., and POLANYI, J. C., 1982, *J. chem. Phys.*, **76,** 913.
[120] BARNES, J. A., KEIL, M., KUTINA, R. E., and POLANYI, J. C., 1980, *J. chem. Phys.*, **72,** 6306.
[121] SUNG, J. P., and SETSER, D. W., 1978, *J. chem. Phys.*, **69,** 3868.
[122] ANDRESEN, P., JOSWIG, H., PAULY, H., and SCHINKE, R., 1982, *J. chem. Phys.*, **77,** 2204.
[123] NIELSON, G. C., PARKER, G. A., and PACK, R. T., 1977, *J. chem. Phys.*, **66,** 1396.
[124] NESBITT, D. J., NIBLER, J. W., SCHIFFMAN, A., CHAPMAN, W. B., and HUTSON, J. M., 1993, *J. chem. Phys.*, **98,** 9513.
[125] SCHIFFMAN, A., CHAPMAN, W. B., and NESBITT, D. J., in preparation.
[126] CHAPMAN, W. B., SCHIFFMAN, A., NESBITT, D. J., and HUTSON, J. M., in preparation.
[127] BUCK, U., KOHLHASE, A., PHILLIPS, T., and SECREST, D., 1983, *Chem. Phys. Lett.*, **98,** 199.
[128] BUCK, U., KOHLHASE, A., SECREST, D., PHILLIPS, T., SCOLES, G., and GREIN, F., 1985, *Molec. Phys.*, **55,** 1233.
[129] BUCK, U., KOHL, K. H., KOHLHASE, A. FAUBEL, M., and STAEMMLER, V., 1985, *Molec. Phys.*, **55,** 1255.
[130] MEYER, H., 1994, *J. chem. Phys.*, **101,** 6686.
[131] SCHLEIPEN, J., and TER MEULEN, J. J., 1991, *Chem. Phys.*, **156,** 479.
[132] SCHLEIPEN, J., and TER MEULEN, J. J., 1992, *Chem. Phys.*, **163,** 161.
[133] VAN DER SANDEN, G. C., WORMER, P. E. S., VAN DER AVOIRD, A., SCHLEIPEN, J. J., and TER MEULEN, J. J., 1992, *J. chem. Phys.*, **97,** 6460.
[134] SCHLEIPEN, J. J., and TER MEULEN, J. J., 1993, *Chem. Phys.*, **171,** 347.
[135] CHEUNG, A. C., RANK, D. M., TOWNES, C. H., THORNTON, D. D., and WELCH, W. J., 1968, *Phys. Rev. Lett.*, **21,** 1701.

[136] CHEUNG, A. C., RANK, D. M., TOWNES, C. H., KNOWLES, S. H., and SULLIVAN, W. T., 1969, *Astrophys. J.*, **157,** L13.
[137] CHEUNG, A. C., RANK, D. M., TOWNES, C. H., THORNTON, D. D., and WELCH, W. J., 1969, *Nature*, **221,** 917.
[138] DAGDIGIAN, P. J., 1994, *Experimental Studies of Rotationally Inelastic, State Resolved Collisions of Small Molecular Free Radicals*, in *Chemical Dynamics and Kinetics of Small Radicals*, edited by K. Liu and A. Wagner (Singapore: World Scientific).
[139] REID, M. J., and MORAN, J. M., 1982, *Rev. mod. Phys.*, **54,** 1225.
[140] ANDRESEN, P., ARISTOV, N., BEUSHAUSEN, V., HAUSLER, D., and LULF, H. W., 1991, *J. chem. Phys.*, **95,** 5763.
[141] GWINN, W. D., TUNER, B. E., GOSS, W. M., and BLACKMAN, G. L., 1973, *Astrophysics J.*, **179,** 789.
[142] SHAPIRO, M., and KAPLAN, H., 1979, *J. chem. Phys.*, **71,** 2182.
[143] DEWANGAN, D. P., and FLOWER, D. R., 1983, *J. Phys.* B, **16,** 2157.
[144] DEWANGAN, D. P., and FLOWER, D. R., 1981, *J. Phys.* B, **14,** 2179.
[145] ANDRESEN, P., HAUSLER, D., and LULF, H. W., 1984, *J. chem. Phys.*, **81,** 571.
[146] ANDRESEN, P., 1986, *Comments atom molec. Phys.*, **18,** 1.
[147] GREEN, S., and ZARE, R. N., 1976, *Chem. Phys.*, **7,** 62.
[148] KLAR, H., 1973, *J. Phys.* B, **6,** 2139.
[149] ALEXANDER, M. H., 1982, *J. chem. Phys.*, **76,** 5974.
[150] KOCHANSKI, E., and FLOWER, D. R., 1981, *Chem. Phys.*, **57,** 217.
[151] WALCH, S. P., and DUNNING, T. H., 1980, *J. chem. Phys.*, **72,** 1303.
[152] SONNENFROH, D. M., MACDONALD, R. G., and LIU, K., 1991, *J. chem. Phys.*, **94,** 6506.
[153] DAVIS, S. L., and ALEXANDER, M. H., 1983, *J. geophys. Res.*, **78,** 800.
[154] COREY, G. C., and MCCOURT, F. R., 1983, *J. phys. Chem.*, **87,** 2723.
[155] ALEXANDER, M. H., 1985, *Chem. Phys.*, **92,** 337.
[156] COREY, G. C., and SMITH, A. D., 1985, *J. chem. Phys.*, **83,** 5663.
[157] ALEXANDER, M. H., SMEDLEY, J. E., and COREY, G. C., 1986, *J. chem. Phys.*, **84,** 3049.
[158] MACDONALD, R. G., and LIU, K., 1989, *J. chem. Phys.*, **91,** 821.
[159] MACDONALD, R. G., and LIU, K., 1990, *J. chem. Phys.*, **93,** 2431.
[160] ALEXANDER, M. H., and DAGDIGIAN, P.J., 1994, *J. chem. Phys.*, **101,** 7468.
[161] SCHINKE, R., 1981, *J. chem. Phys.*, **75,** 5449.
[162] MACDONALD, R. G., and LIU, K., 1991, *J. phys. Chem.*, **95,** 9630.
[163] MACDONALD, R. G., and LIU, K., 1992, *J. chem. Phys.*, **98,** 3716.
[164] SCHREEL, K., SCHLEIPEN, J., EPPINK, A., and TER MEULEN, J. J., 1993, *J. chem. Phys.*, **99,** 8713.
[165] SERRI, J. A., MORALES, A., MOSKOWITZ, W., PRITCHARD, D. E., BECKER, C. H., and KINSEY, J. L., 1980, *J. chem. Phys.*, **72,** 6304.
[166] SERRI, J. A., BECKER, C. H., ELBEL, M. B., KINSEY, J. L., MOSKOWITZ, W., and PRITCHARD, D. E, 1981, *J. chem. Phys.*, **74,** 5116.
[167] MOSKOWITZ, W., STEWART, B., BILOTTA, R. M., KINSEY, J. L., and PRITCHARD, D. E., 1984, *J. chem. Phys.*, **80,** 5496.
[168] GOTTWALD, E., BERGMANN, K., and SCHINKE, R., 1987, *J. chem. Phys.*, **86,** 2685.
[169] ZEIGLER, G., KUMAR, S. V. K., RUBAHN, H.-G., KUHN, A., SUN, B., and BERGMANN, K., 1991, *J. chem. Phys.*, **94,** 4252.
[170] BUCK, U., HUISKEN, F., SCHLEUSENER, J., and SCHAFER, J., 1980, *J. chem. Phys.*, **72,** 1512.
[171] BUCK, U., 1982, *Faraday Disc. Chem. Soc.*, **73,** 187.
[172] BUCK, U., HIUSKEN, F., OTTEN, D., and SCHAEFER, J., 1983, *J. chem. Phys.*, **78,** 4439.
[173] ANDRES, J., BUCK, U., HUISKEN, F., SCHLEUSENER, J., and TORELLO, F., 1980, *J. chem. Phys.*, **73,** 5620.
[174] SCHAEFER, J., and MEYER, W., 1979, *J. chem. Phys.*, **70,** 344.
[175] FAUBEL, M., RUSIN, L. Y., SCHLEMMER, S., SONDERMANN, F., TAPPE, U., and TOENNIES, J. P., 1993, *J. Chem. Soc. Faraday Trans.*, **89,** 1475.
[176] MALIK, D. J., SECREST, D., and BUCK, U., 1980, *Chem. Phys. Lett.*, **75,** 465.
[177] BUCK, U., SCHLEUSENER, J., MALIK, D. J., and SECREST, D., 1981, *J. chem. Phys.*, **74,** 1707.
[178] CHANDLER, D. W., and HOUSTON, P. L., 1987, *J. chem. Phys.*, **71,** 1445.
[179] STRICKLAND, R. N., and CHANDLER, D. W., 1991, *Appl. Optics*, **30,** 1811.

[180] SUITS, A. G., BONTUYAN, L. S., HOUSTON, P. L., and Whitaker, B. J., 1992, *J. chem. Phys.*, **96,** 8618.
[181] BONTUYAN, L. S., SUITS, A. G., HOUSTON, P. L., and WHITAKER, B. J., 1993, *J. phys. Chem.*, **97,** 6342.
[182] WEIDA, M. J., and NESBITT, D. J., 1994, *J. chem. Phys.*, **100,** 6372.
[183] KHARE, V., KOURI, D. J., and HOFFMAN, D. K., 1982, *J. chem. Phys.*, **79,** 4493.
[184] MATTHEUS, A., FISCHER, A., ZIEGLER, G., GOTTWALD, E., and BERGMANN, K., 1986, *Phys. Rev. Lett.*, **56,** 712.